DETERMINATION OF THE DEGREE OF MIXING OF CERAMIC POWDERS BY RAMAN SCATTERING

BY

AMIT SRIVASTAVA

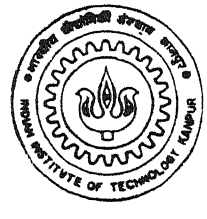

MATERIALS SCIENCE PROGRAMME

INDIAN INSTITUTE OF TECHNOLOGY KANPUR

JULY, 2000

DETERMINATION OF THE DEGREE OF MIXING OF CERAMIC POWDERS BY RAMAN SCATTERING

A Thesis submitted
in partial fulfillment of the requirement
for the Degree of

Master of Technology

by

Amit Srivastava

Materials Science Programme
INDIAN INSTITUTE OF TECHNOLOGY, KANPUR
JULY 2000

CERTIFICATE

It is certified that the work contained in this thesis entitled **"Determination of Degree of mixing of Ceramic Powders by Raman Scattering" by Amit Srivastava (Roll no. 9811201)** has been carried out under our supervision and this work has not been submitted elsewhere for a degree.

(Asima Pradhan)
Asstt. Professor

Department of Physics &
Center for Laser Technology
Indian Institute of Technology
Kanpur 208016,India

(D.C.Agrawal)
Professor

Materials Science Programme
Indian Institute of Technology
Kanpur 208016,India

Dedicated
To
My Papa

Acknowledgement

I am deeply indebted to Prof. D.C. Agrawal and Dr. Asima Pradhan for their inspiring guidance. I am very fortunate as I had been under their tutelege. Both constantly encouraged me and the freedom I got was absolutely remarkable. I wish to take their valuable advices which I sure, will help me to eradicate many troubles in future.

I also express my sincere acknowledgement to my teachers Dr Jitendra Kumar, Dr.K.Shahi, Dr. K.N.Rai, Dr. Y.N.Mohalpatra and Dr.Om Prakash for introducing me to fundamental concept of materials Science and for encouraging us to participate in useful discussions.

I express my deep indebtness to my friends D.K.Rai, K.K.M.Pandey and Shyam for their moral support and encouragement during my stay in IIT. Discussion with them ,though sometimes led to serious attraction have helped me to get out of my troublesome moments and bitter experience in IIT.Inspite of their busy schedule, Sharad Gupta and Maya di helped me a lot in the experiment mainly during recording Raman Spectra of my samples. I thank him again and again

.I am thankful to my classmates Mini , Ramanujam, Saibaba and Srikant for maintaining a cordial and friendly environment throughout the course work period and theirafter.I would like to extend my sincere thanks to my lab mates Santosh,Sarika,Animesh,Sreya and Niraj for their pleasant approach. I appreciate Mr.G.S.Thapa for his timely and selfless help and also his encouraging attitude .I am grateful to the staff member of ACMS for their technical and nontechnical help in the present work.

I am also thankful to my lovely friends Chandan, Rajan, Anil, Ajay, Abhishek,Ravi, Shivgovind , Alok and Shatish who made my stay at IIT a memorable one.

The silent support from my family members was always a constant source of inspiration for me during my stay.

Amit Srivastava

Abstract

Multicomponent oxide ceramics are usually prepared by mixing the powders of different oxides and then subjecting this mixture to calcination, sintering and other operations. A homogeneous mixing of the powders is essential to obtain a product with uniformity of composition and free from defects. Many methods such as mixing in a ball mill or other mechanical devices, colloidal mixing etc., are employed to achieve a uniform mixing with different efficiencies. mixedness of powders is very important parameter in ceramic processing. In the present work, Raman spectroscopy has been used to evaluate the degree of the mixing of TiO_2 and ZrO_2 powders. Mixing was carried out by mixing the two powders in different volume ratios either by dry mixing or by first preparing an aqueous suspension of each powder, mixing these suspensions and drying. The pH of the suspensions were varied to vary the degrees of dispersion of the powder .The mixtures were examined either as loose powders or as pellets. The Raman spectra were obtained at two beam sizes of 2μm and 10μm respectively. The volume fractions of the constituents in the mixture were extracted by fitting the Raman spectra of the mixture to a linear combination of the spectra from the pure powders. The spatial variation in composition of titania was found to be much higher in the dry mixed samples as compared to the mixtures prepared from suspensions. This indicated that better mixing is obtained

from suspensions. Best mixing was obtained when the pH of the starting suspensions were 6 and 9 for ZrO_2 and TiO_2 respectively. The scatter in the results is considerably reduced by using 10μm beam size (instead of 2μm beam size) and a suitable sample holder. The concentration of TiO_2 was consistently above and consistently below the actual concentration for the loose powder samples and the pellets respectively. An explanation for the observation is presented and avenues of future work as indicated.

CONTENTS

CHAPTER – 2

CHAPTER –3

CHAPTER –4

LIST OF FIGURES :

CHAPTER 1

CHAPTER-2

CHAPTER-3

CHAPTER 1
INTRODUCTION

1.1 INTRODUCTION

Speaking after receiving the Nobel Prize in Physics in the year 1930, on December 11, Raman said [1]

"The universality of this phenomenon, the convenience of the experimental technique and the simplicity of the spectra obtained enable the effect to be used as an experimental aid to the solution of wide range of problems in physics and chemistry. Indeed it may be said that it is this fact which constitutes the principal significance of the effect, the frequency difference determined from the spectra, the width and character of the lines appearing in them, the intensity and the state of the polarization of the scattered radiation enable us to obtain an insight into ultimate structure of the scattering substance. As experimental research has shown that these features in the spectra are definitely influenced by physical condition such as mixture, solution, molecular association and polymerization it follows that the new field of spectroscopy has practically unrestricted scope in the study of the problems reaching to the structure of matter. We may also hope that it will lead us to a further

understanding of the nature of the light and of the interaction between the matter and the light."

Really we can say that History has proved him right. The Raman Scattering method of investigation produces a distinct spectrum from materials and has opened up an entirely new and broad field of study of molecular structure and other applications.

1.1.1RAMAN EFFECT

Raman effect is concerned with the phenomenon of a change of frequency when light is scattered by a molecule. In 1928 Raman discovered that molecular scattering of monochromatic radiation produces not only scattered radiation of unchanged frequency (Rayleigh Scattering), but also a small portion of scattered radiation of different frequencies (Raman Scattering). It may be regarded as an inelastic collision between an incident photon and a molecule where a quantum of the molecular rotational, vibrational or electronic energy is either absorbed or emitted as a result of collision. The difference in frequency between the incident radiation and that of Raman-scattered radiation is known as Raman frequency shift. The magnitudes of the various Raman-shifts observed for a particular sample are a property of the sample and are independent of the excitation frequency.

1.1.2CLASSICAL THEORY OF RAMAN EFFECT

The Raman effect, may to some extent, be explained on the basis of the classical theory. Consider an electromagnetic radiation incident upon a diatomic molecule. Three of the many possible orientations of the

molecules with respect to the incident radiation have been shown in figure 1.1

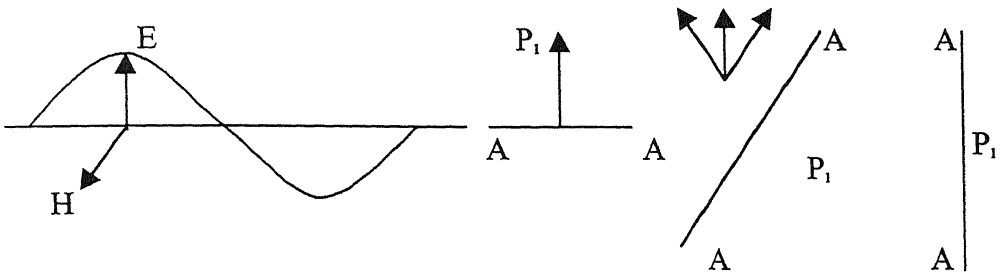

Fig 1.1: Possible orientations of the molecule with respect to the incident beam

If the frequency of the incident radiation is markedly different from the frequency of any absorption band in the spectrum of the molecule, then the oscillating field $\vec{E}$ will induce the electrons in A-A bond to oscillate in phase. This leads to an oscillating dipole moment in the molecule A-A. The magnitude and direction of the induced dipole moment is given to a first approximation by

$$P_i = \alpha E \quad \text{.....(1.1)}$$

where α is the polarizability of the molecule. Polarizabililty is a measure of the ease with which an electron follows an electric field. E is the amplitude of the electric field vector of the incident radiation.

If a diatomic molecule is vibrating with a frequency ν_e, it may be assumed that the polarizability will vary in a harmonic manner and will therefore vary with time according to the expression

$$\alpha = \alpha_o + b \sin 2\pi\nu_e t \quad \text{.....(1.2)}$$

where α_o and b are constants and t is time.

The oscillatory field E is chosen to occur at a much larger frequency ν than ν_e. The magnitude of the field as a function of time is given by

$$E = E_o \sin 2\pi\nu t \quad \text{.....(1.3)}$$

where E_o is the peak amplitude of the oscillating field.

Then the expression for the variation with time of magnitude of the dipole moment induced in the molecule can be obtained using eq.(1.1-1.3) as

$$P_i = \alpha_o E_o \sin 2\pi\nu t + b E_o \sin 2\pi\nu t \sin 2\pi\nu_e t \quad \text{.....(1.4)}$$

The equation can be reduced using trigonometrical relations

$$P_i = \alpha_o E_o \sin 2\pi\nu t + \tfrac{1}{2} bE_o[\cos 2\pi(\nu - \nu_e)t + bE_o[\cos 2\pi(\nu + \nu_e)t] \quad \text{.....(1.5)}$$

This equation indicates that the emitted radiation will have components with ν, $(\nu + \nu_e)$, $(\nu - \nu_e)$. The spectrum of the emitted radiation will contain three bands or lines at these frequencies and are referred to as Rayleigh, Raman (Stokes) and Raman (Antistokes) lines respectively.

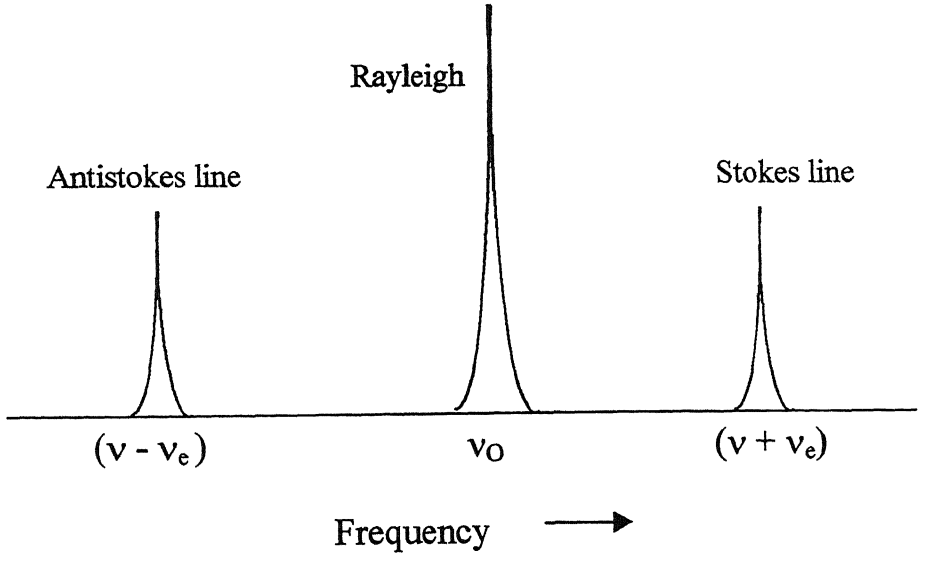

Fig (1.2): Spectrum of scattered radiation

1.1.3. QUANTUM THEORY OF RAMAN EFFECT

The occurrence of Raman scattering may be understand more easily in terms of quantum theory of radiation. Consider a diatomic molecule in one or other of the two lowest vibrational energy levels E_0 and E_1. In quantum terms an incident photon possesses energy ε_i given by the expression

$$\varepsilon_i = h\nu_i \quad \text{.....(1.6)}$$

where ν_i is the frequency of the incident radiation.

On collision, the photon may perturb the molecule and the total combined energy of the molecule and photon, E_T, at the moment of collision is given by

$$E_T = \varepsilon_i + E_v \quad \text{.....(1.7)}$$

Where E_v is either E_1 or E_0

The energy of the photon scattered as a result of the collision with the sample molecule is given by

$$\varepsilon_s = h\nu_s \quad \text{.....(1.8)}$$

where ν_s is the frequency of the incident radiation.

The process can occur in four possible ways, two of which correspond to elastic and the other two to inelastic collisions.

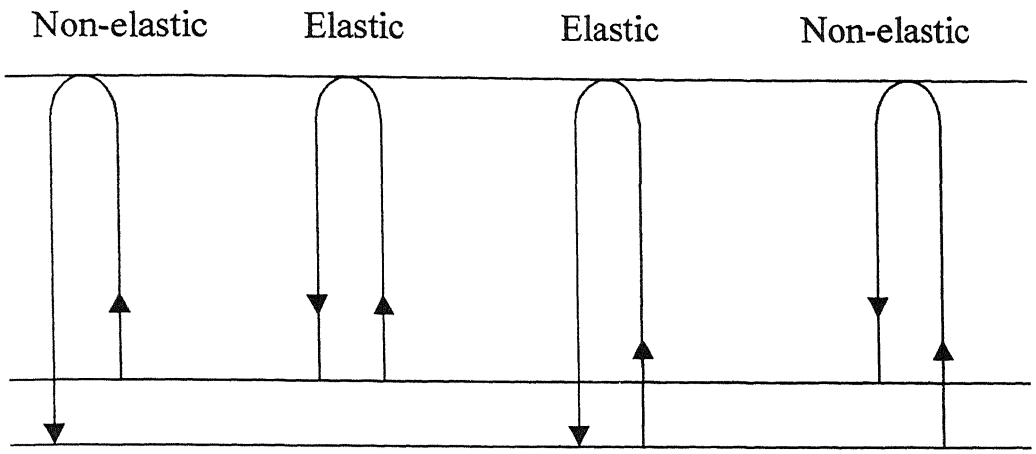

Fig (1.3): Change in frequency during different scattering phenomenon

The magnitude of Raman shift is related to difference in energy between two levels E_0 and E_1. If the molecule is considered to be an anharmonic oscillator, the Raman shifts in units of cm^{-1} will be given as

Stokes $\Delta\nu = \nu_i - \nu_s = \nu_e (1-2x_e)$

Antistokes $\Delta\nu = \nu_s - \nu_i = \nu_e (1-2x_e)$

where x_e is the anharmonicity constant.

In Raman spectroscopy, only Stokes lines are usually measured. Antistokes lines involve transition from excited vibrational – rotational states of the sample. The population of these states is very much less than the population of the ground states; therefore very few molecules are available to give up quantum of vibrational energy and so it is customary to measure the Stoke's lines in Raman experiment.

Raman scattering phenomenon can be pictured in terms of a ball striking a drum. If the surface of the drum is stationary, when the ball hits it will start oscillating at its own frequency and the ball will be reflected with less frequency, having lost an amount of energy that is taken up by the oscillation of the drum. On the other hand, if the drum is already oscillating and the ball hits the drum at right phase of the drum's oscillation, the drum will give energy to the ball and the ball will be flung off with increased energy.

1.1.4 APPLICATION OF RAMAN SCATTERING IN MATERIALS SCIENCE

Raman Spectroscopy has wide ranging applications in chemical, physical, biological, medical and materials sciences. Such applications vary from the purely qualitative to highly quantitative. Quite often, Raman Spectroscopy is used simply to identify the chemical species.

Modern materials science requires techniques for processing and characterization of materials. Molecular probes such as Raman spectroscopy are some of the most valuable tools for determining molecular structure particularly when it is supplemented by imaging to obtain spatially resolved compositional information of inhomogeneous or low volume samples. Now a days, Raman spectroscopy is widely used in materials science to understand the phase transformation in materials. Some more applications of Raman spectroscopy in materials science are described in the following paragraphs.

- The Raman peaks of crystalline semiconductors are sharp because of the well-defined wave vector of the phonon. This is a direct

consequence of momentum conservation. Disorder in the crystals (defects) or small crystalline size – down to amorphicity, results in an asymmetrical peak broadening and a shift to the lower frequencies. As a result, the Raman spectrum offers direct information on the crystallinity of the sample. Fig (1.4) shows the difference in the spectra obtained for crystalline silica (c-Si), polycrystalline silica (p-Si) and amorphous silica (a- Si) [2]. It is clear that the Raman Spectroscopy is a powerful tool to infer the crystal structure of materials.

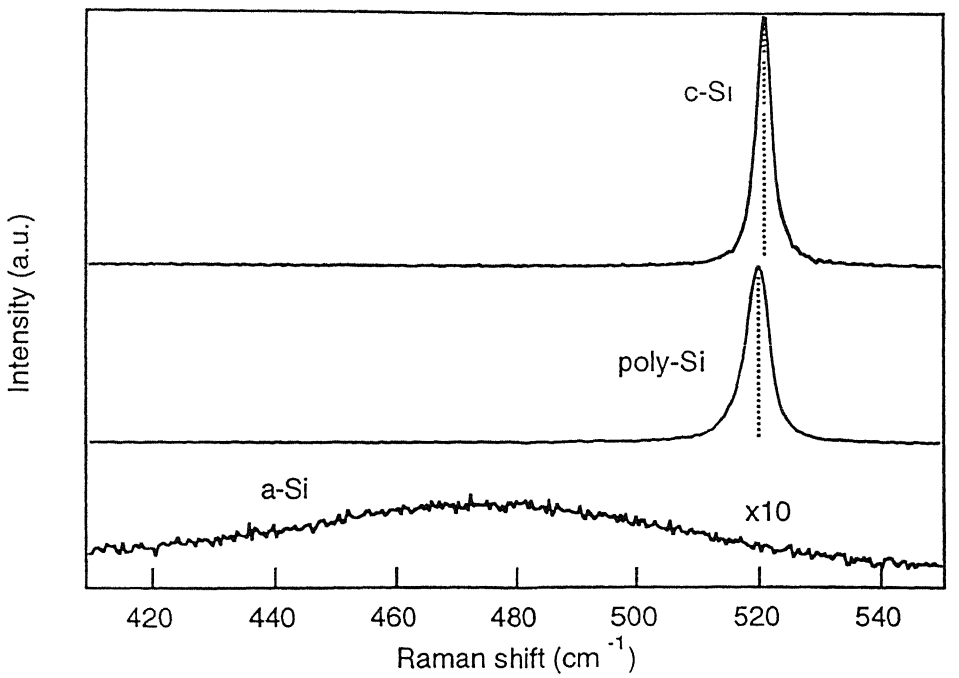

Fig (1.4) Raman signal of crystalline silica (C-Si), polycrystalline silica (Poly-Si) and amorphous silica (O-Si)

- Raman scattering of a molecule provides a spectroscopic technique for the identification of the symmetries of the structure and bonding of carbons and energies associated with these fundamental excitations in the various forms of carbon. Carbon is known to form single, double and triple bonds, resulting in linear chains, strongly anisotropic layered materials, and three dimensional solids and novel molecular based solids based on periodically positioned spherical or cylindrical carbon shells respectively. The large differences in the Raman spectra of various forms of carbon including graphite, fullerenes and carbon nanotubes make the Raman technique useful for distinguishing one form of carbon from another[3]. In addition, Raman techniques have also been successfully applied to study unique one-dimensional aspects of the vibrational spectra of carbon nanotubes. Carbon nanotubes have attracted the attention of the scientific community because of the prediction that about one third of the nanotubes are metallic and rest are semi conducting depending upon the nanotube diameter.

- The use of Raman Spectroscopy in the petroleum industry is widespread, concerned with the characterization of additives and catalysts used in the production of gasolines and fuels.[4] However recently the use of Raman Spectroscopy as an analytical tool for monitoring the composition of fuels for both process control and quality control applications has been gaining ground.[5] The advantages of using a rapid spectroscopic method which provides detailed chemical information in order to evaluate these fuels

become apparent when one considers how slow and tedious are the traditional methods for monitoring the fuel composition and quality.

- Nanosized TiO_2 has a very significant application as a dye-sensitized photo anode in new types of solar cells. Raman scattering can be used to determine the particle size of the sol gel synthesized TiO_2, which shows good agreement with the particle size determination using XRD.[6]

- Raman spectroscopy has been used to study the thermal degradation of ceramic fibers embedded in a refractory glass ceramic material which can exhibit enhanced toughness through a specific micro-mechanism at the fiber matrix interface.[7]

- Raman spectra have been used to identify the phases of TiO_2 at different temperatures to monitor the transformation of the structure in a small temperature range and also to monitor the phases before and after transformation. TiO_2 is one of the ceramic powders that are widely used and its structure is interesting and important. Thermo Raman spectroscopy has been used to monitor the phase transformation from xerogel, prepared by sol gel method, by sintering at different temperatures. Various phases or mixtures of xerogel, amorphous TiO_2, anatase and rutile have been at different sintering temperatures.[8] Observed fluctuations in intensity were observed. These might be because of the rearrangement in structure during the transformation from one phase to another.

The thermo-Raman data showed that the aging period of xerogel is important when preparing anatase or rutile. The freshly prepared xerogel formed anatase but the aged xerogel gave rutile. Thus Raman spectroscopy can be used to monitor the phase transformation of ceramics at various temperatures.

- The investigation of the optical properties of crystalline germanates such as $Bi_4Ge_3O_{12}$ (BGO) is of interest because of their use as laser materials. Raman spectroscopy plays an important role in the determination of the optical phonon modes and phase transition in the $Bi_4Ge_{3-x}Ti_xO_{12}$ system.[9]

- Binary and ternary Telluride glasses are extensively studied because of their promising electrical and optical properties such as their high refractive index, wide infrared transmittance and high dielectric constant. In many conducting ion glasses it has been observed that partial substitution of one network former by another results in glasses with higher conductivity. Raman spectroscopy is used to study the structure dependence on the composition and temperature and their crystallization behavior. [10]

- Raman spectroscopy is a useful tool for the characterization of a gas phase, especially in systems in which there are gradients of temperature or composition.[11]

- High T_c superconductors have been investigated by Raman scattering both from interest in their fundamental properties and

from the point of view of characterizing them for applications. $YBa_2Cu_3O_{7-\delta}$ is a widely used superconducting material. Raman scattering is a powerful tool for investigation of such complex phenomenon in $YBa_2Cu_3O_{7-\delta}$ as micro phase separation and reordering process. Raman scattering may help significantly the efforts to explain the structural background of high T_c superconductors.[12]

- Raman spectroscopy has been successfully used to investigate the nature of thin films prepared by sol-gel technique. Lead Zirconia Titanate (PZT) is a well-known solid solution. Thin films of PZT prepared by sol-gel technique on sapphire and fused quartz substrate have different structure that are confirmed by Raman spectroscopy.[13] On sapphire the films crystallize into the perovskite structure whereas on fused quartz they form pyrochlore. Fig (1.5) shows the Raman spectra of PZT and fig (1.6) shows the background subtracted Raman data for PZT films. From the comparison of Raman spectra it is obvious that both powder and film on sapphire substrate belong to perovskite structure whereas the film on fused quartz has a pyrochlore structure. Thus Raman spectroscopy is an elegant technique to know the structure of the thin films prepared by sol-gel technique.

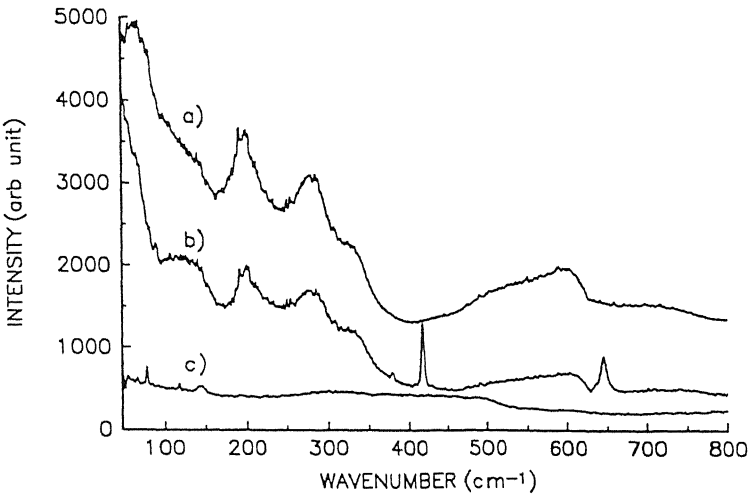

Fig (1.5) Raman spectra of PZT a) powder, b) film on sapphire substrate, c) film on quartz substrate [13]

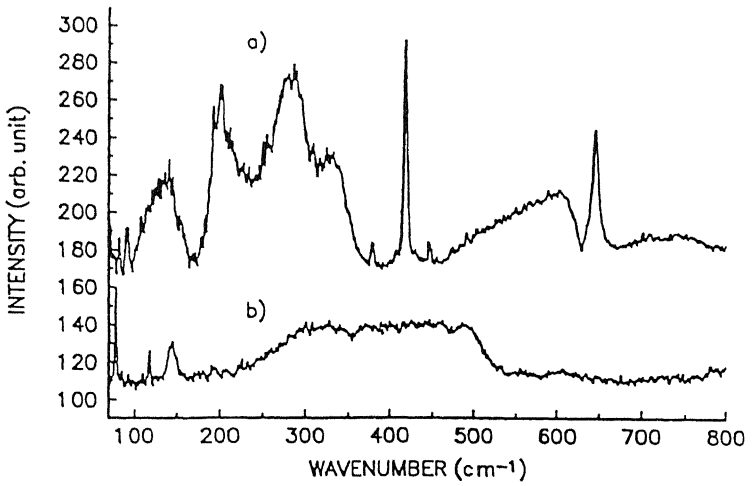

Fig (1.6) background subtracted Raman spectra of PZT film on a a) sapphire, b) quartz substrate [13]

1.2 IMPORTANCE OF POWDER MIXING IN CERAMIC PROCESSING

Mixing of the constituent powders is a critical step in the preparation of multicomponent ceramic bodies. Mixing of powders is also of great concern in several other industrial processes in order to achieve the desired physical and chemical properties. Particle components in a powder mixture do not usually have identical properties and differ in physical characteristics. Mixing of such components can produce segregation that prevents the formation of a perfect mixture. A uniform mixing is desired to avoid the spatial variations in compositions as well as to produce components with good sintered density free of voids and other flaws. The scale of homogeneity in solid particulate mixture is of critical importance in diverse set of applications in advanced ceramics. Homogeneity of a mixture affects the sintering process, the final or pre-final manufacturing operation in the production of ceramics. If the mixture is not homogeneous, the pressing step used in pellet formation causes some regions to have more green density than others. Inhomogeneous sintering and shrinkage may occur in materials containing relatively dense packed regions or regions containing finer particles that are separated by more porous regions containing larger particles. Regions containing smaller pores or particles that densify earlier may precede the more porous region into the final stage of sintering and the coarser pores in the boundary region tend to persist.

1.3 GENERAL REMARKS ON MIXING

Mixing is a rather loosely defined term. In general, a mixture is defined as a blend of two or more ingredients that, no matter how finely commingled, retain separate identities. In a particulate mixture one type of particle can always be distinguished from another and differences can be used to measure the effectiveness of mixing. The degree of mixing can be described in terms of a scale of segregation,[14] which is the length scale of physical separation between components in a mixture. Another way to view mixing is in terms of compositional homogeneity.

Ideally the purpose of mixing operation is to obtain a distribution in which each particle of a constituent is near a particle of another constituent. This is called an ideally ordered mixing.[15] A schematic representation is shown in fig (1.7a) and is compared with a perfectly random mixture in fig(1.7b).

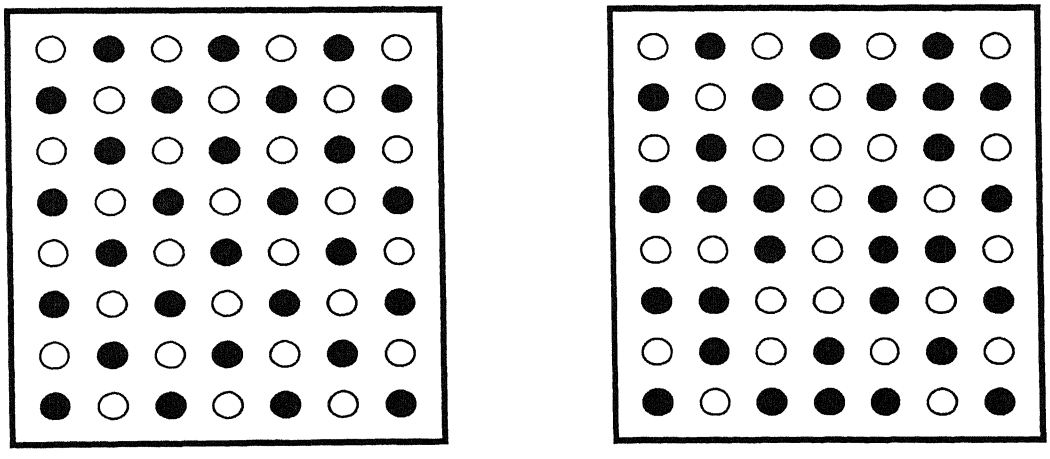

Fig 1.7 a) Ideally ordered mixture b) Perfectly random mixture

The probability of obtaining such a mixture in industrial mixtures is zero.

The terms ordered and random mixing is introduced to evaluate the commercial reality. Randomization requires particles of equal size and weight with little or no surface effects. Ordered mixing is considered to be different from random mixing since it does not require equal sized or weighed particles but rather particle interactions i.e. absorption, chemisorption or any form of adhesion. The concept is applied to cohesive or interacting fine particles. Ordered mixing is observed when a small proportion of fine particles adhere to coarser particles of second constituent. If mixing is complete, this may result in a coating of fine particles on the coarser constituent.

The concept of ordered and randomized mixtures have been improved in order to give more information on the nature of mixing. Le – Lan suggested a partially random mixture as a mixture in which the probability of finding a constituent at every point is identical.[16] A non-random binary mixture was defined as one in which the probability of finding a particle of one component is not constant throughout the mixture.

1.3.2 SCALE OF SEGREGATION

The degree of mixing can be described in terms of the scale of segregation, which is the length scale of physical separation between components in a mixture. The homogenization procedure always occurs in competition with segregation or a demixing process and this secondary phenomenon prevents perfect mixing from being obtained. The final state reached is an equilibrium, which can be visualized as a reversible process

Segregation ⟷ Mixing

The mixing quality depends directly on this dynamic equilibrium.

Demixing basically arises

➔ by separation of the components induced by difference in particle size, shape and density.

➔ by agglomeration of the particles; the factors which can induce agglomeration include humidity and electrostatic charges.

The difference in particle size is the most important factor leading to segregation. The length of segregation depends on the particle size as[17]

$$d = \frac{v_o D^2 \eta}{\rho}$$

where d is the length of segregation

D, the particle size, η, viscosity of the medium and ρ is the density of the material.

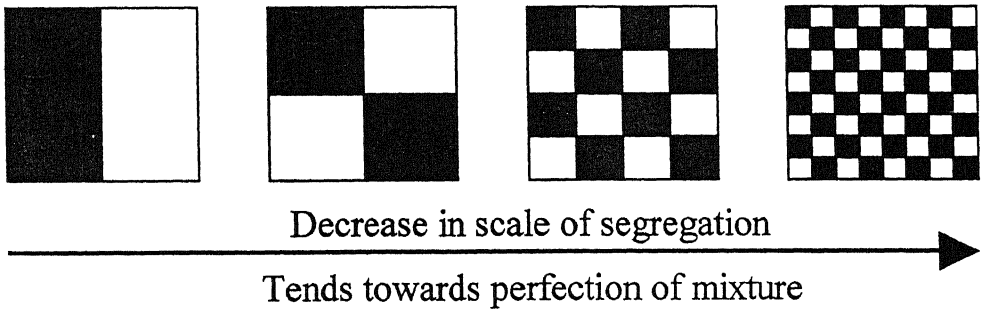

Fig 1.8: Diagrammatic relation between segregation and mixedness

1.3.3SCALE OF HOMOGENEITY

This is another way to view the mixing. A mixture can be defined as homogeneous, if the probability of finding particles of any particulate

component at any point throughout the mixture is same, if it is not so then the mixture is said to be inhomogeneous. The scale of homogeneity is an important way to find the spatial voids, defects etc.

1.3.4POWDER MIXING MECHANISM

The mixing of the powders proceeds mainly in three ways:

1. **Mixing by convection**: This type of mixing is characterized by the movement of groups of particles within the mixture. The components are divided into clumps. They are displaced relative to one another and the sizes of clumps get reduced by the process. This motion creates contact area between different components. This mechanism operates during mixing on a large scale. Flow produced by stirring contributes importantly to convection mechanism.

2. **Mixing by diffusion:** This type of mixing occurs by the motion of individual particle, to ensure the mixing on a fine scale. In this process, there is an interchange of molecules and particles randomly between neighboring regions in the mixture.

3. **Mixing by shear:** Mixing occurs by slipping of particles within the whole volume. This mechanism is often considered to be a combination of the other two processes. The schematic representation of the mixing mechanism is shown in the Fig.(1.9).

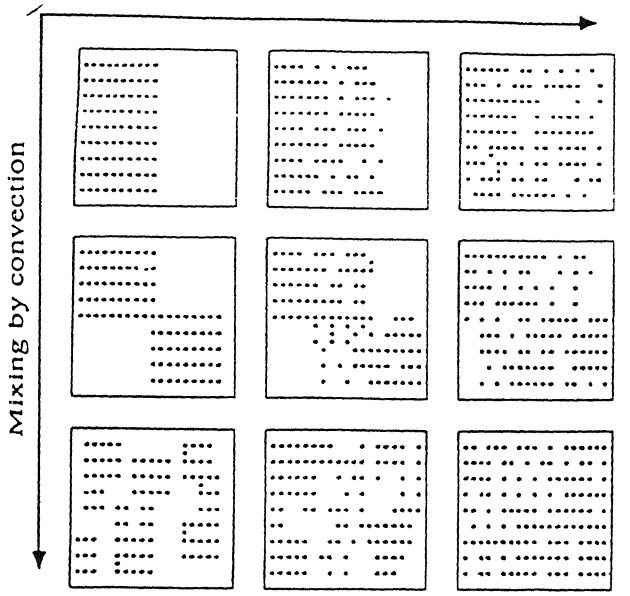

Fig 1.9: Schematic representation of mixing mechanism

1.4 USE OF RAMAN SPECTROSCOPY TO CHARACTERIZE THE DEGREE OF MIXING

Raman scattering is normally linearly related to the concentration of the scattered species and also it depend on the molecular weight of the species as [18]

$$I = C\, I_0\, \alpha\, \nu_s^4$$

where α depends on the molecular weight.

Raman shift is the characteristic of any material. Raman spectra of the mix pattern of the constituent powder can be overlapped with the linear combination of their pure constituent powder's spectra. Thus we can have an idea of the compositional fraction of the corresponding pure powders in the mixture one, here the spectra of pure powders were collected under the same condition such as same power with same laser spot size as used for the mixture samples and the intensity of the spectra scattered by each of the two constituents is proportional to the total surface that it present to the incident laser beam. The area thus determined are equal to the volume fractions of the powders, so we can say that Raman spectroscopy is a valid procedure to determine the degree of mixing or homogeneity of the mixture.

1.5 MIXING OF CERAMIC POWDER IN LIQUID SUSPENSION

In the present work, our aim is to use Raman spectroscopy to see if it can determine the degree of mixing. For this purpose, samples are needed with different degree of mixing. Apart from the mixing in dry state, the suspension of the powders can be mixed also. The ceramic powders can be dispersed or flocculated in a liquid depending on the conditions such as pH of the liquid. The state of the dispersion can be controlled by single means such as changing the chemistry (pH, additives) of the suspension. Then by mixing, suspension containing the solid phase in different degree of dispersion, the mixing of the powders can be changed. This is the technique adopted in the present work to prepare the samples with different degree of mixing .In the following

section we discuss briefly the mechanism responsible for the state of dispersion of ceramic powders.

1.5.1THEORY OF FLOCCULATION AND DEFLOCCULATION

During many ceramic-processing steps, it is necessary to incorporate a powder into a liquid medium such that the particles are evenly dispersed. If the powder surface is lyophobic, the powder is difficult to be dispersed; if it is lyophilic the powder disperses easily (for water dispersion, the term hydrophobic and hydrophilic are used respectively.). Dispersing agents are therefore, added to wet the surface of hydrophobic materials to make them hydrophilic. Dispersion stabilized by an additive adsorbed on the particles, which increases the repulsion forces by electrical charging, is called deflocculating. Polymer electrolytes of low molecular weight may be powerful deflocculants in the systems containing polar liquids. A coagulant is a simple electrolyte that promotes particle agglomeration by reducing the particle repulsion forces. Particle agglomeration may also be produced by the bridging action of some of the adsorbed polymer molecules and coagulated colloidal particles. This type of agglomeration is called flocculation.

1.5.2 PARTICLE CHARGING IN LIQUID SUSPENSION

Ceramic powders are of high surface area and relatively low solubility and surface chemistry tends to control their charging behavior. The surface of the particle may become charged by a chemical reaction between the surface and the liquid medium changing the composition of the surface.

For oxides with hydrated surface, the surface chemistry in water is dominated by the chemical reactions.

$$MOH_2^{+}(surface) \Rightarrow MOH_{(surface)} + H^{+}_{(solution)}$$

$$MOH_{(surface)} \Rightarrow MO^{-}_{(surface)} + H^{+}_{(solution)}$$

where M represents a metal ion at the surface such as Ba^{+2}, Al^{3+}, Si^{4+}, Ti^{4+}, Zr^{4+} and so on. Each M is also bonded to bulky oxygen ions to satisfy its bonding needs. The charge on a hydrated surface of a pure oxide particles dispersed in water is determined by its reaction with H_3O^{+} or OH^{-} ions. The addition of H_3O ions will reduce the pH and cause the uncharged surface to get protonated and become positively charged. The addition of OH^{-} ions will remove hydrogen from the surface and produce a negative surface charge at large pH. At certain pH, there will no net charge on the surface. This pH is called the "point of zero charge (PZC)" and is given by:

$$PZC = (pK_1 + pK_2)/2$$

An example is illustrated here to explain the above statement.

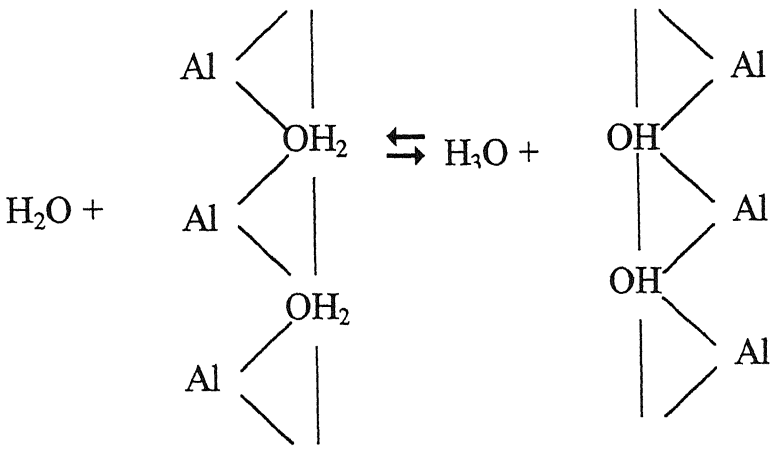

pH < 9 (IEP of Al_2O_3)

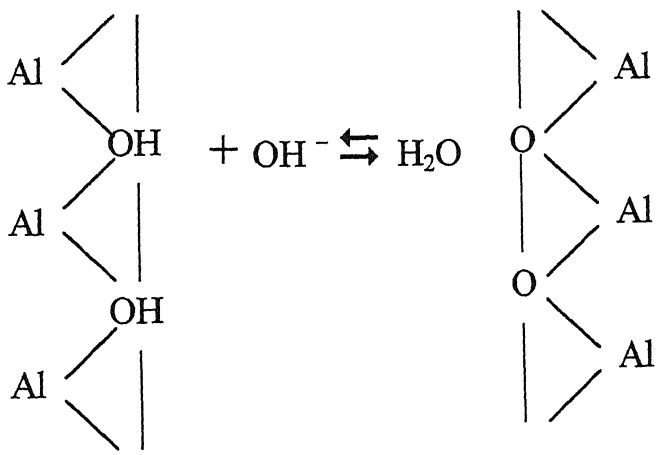

pH > 9 (IEP of Al_2O_3)

1.5 STATEMENT OF THE PROBLEM

A homogeneous mixing of the powders is essential to obtain a product with uniformity of composition and free from defects. Mixedness of a powder mixture is an important parameter in ceramic processing. Raman spectroscopy is an accurate and rapid tool to evaluate the degree of mixing. The objective of the present work has been to study the effect of particle size, laser beam size and technique of mixing (i.e. dry mixing and mixing through aqueous suspension of powders at different pH) on the degree of mixing of ceramic powders (TiO_2 and ZrO_2) determination using Raman spectroscopy.

CHAPTER 2
EXPERIMENTAL PROCEDURE

2.1 SAMPLE PREPARATION

In the present work, we have used TiO_2 and ZrO_2 ceramic powders. These ceramic powders have been chosen as they give distinct Raman spectra with comparable intensities .The properties of these powders are shown in the table below.

Table 2.1: Properties of TiO_2 and ZrO_2 powders

Powder	Manufacturer	Purity (%)	Density gm/cm^3	Melting Point (°C)	Molecular weight (gm)	Structure
TiO_2	Aldrich, USA	99.9	3.90	1855	79.88	Anatase
ZrO_2	MEL, USA	98.5	5.89	2715	123.22	Monoclinic
ZrO_2	TOSOH, JAPAN	98.5	5.89	2715	123.22	Monoclinic

2.1.1 CHARACTERIZATION OF POWDERS

2.1.1.1 PARTICLE SIZE ANALYSIS

Particle size analysis of these powders has been carried out by laser diffraction techniques using a commercial instrument (Fritch Particle sizer analysette 22 Model Economy made in Germany)

2.1.1.2 DETERMINATION OF SURFACE AREA

The surface area of powders is determined by the single point physical adsorption of a gas, using a surface area analyzer (SA 3100,Micromeritics, UK).

2.1.1.3 ISOELECTRIC POINT

The isoelectric points of these powders have been determined by measuring the zeta potential at different pH using an electrophoresis apparatus (Mark II Rank Brothers, UK).

PROCEDURE

A small amount of powder (~0.2 gm) is dispersed in aqueous suspension of different pH (total volume of suspension ≈50 ml) by stirring for nearly 15 minutes, followed by ultrasonication (for 5 minutes). This suspension is nearly transparent with very slight milky appearance. The cell of electrophoresis apparatus is cleaned with distilled water. Sufficient quantity of the prepared suspension is now poured in the cell so that the platinum electrodes can be half immersed. Now the electrodes are inserted in the cell and the microscope is focused to view the stationary level (the distance from the wall, at which the liquid is stationary, due to the balance between the electro-osmotic streaming flow

and the reverse flow at hydrostatic equilibrium which itself obeys Poiseulle's law [ref], for the flat cell used here has been determined to be 0.136 cm from the inner wall of the cell) The inner wall of the cell is first brought into the field of view by moving the micrometer screw. Then the field of view is moved 0.136 cm towards the center of the wall. The temperature of the suspension is controlled to 30°C. The field is now applied and the time for the particle to see crossing a certain number of grids (3 or 4) in the eyepiece is measured. At least 5 such pairs of measurement are taken. The average time is calculated. Using the given value of spacing between the grids (0.0467 mm), and the value of the distance between the electrodes (8.79 cm), mobility and hence zeta potential is calculated. This process is repeated for suspensions of different pH. The potential is calculated using the formula:

$$\xi = \frac{f_H \eta v_e}{\varepsilon_r \varepsilon_o E}$$

where

f_H = Henry constant (3/2)

η = viscosity of water = 8 x 10^{-4} Poise at 30° C

v_e = electrophoretic velocity

ε_r = relative permittivity of the medium

ε_o = permittivity of vacuum

E = applied electric field

Table 2.2: Zeta Potential of Zirconia powder

PH of the solution	Position of the wall (cm)	Time for the particle to cross 4 grids		Average time (second)	Zeta potential (mV)
		When the electrical field is applied in right direction	When the electrical field is applied in left direction		
2	12.736	9.93 9.32 10.32 11.12	9.62 9.35 9.21 9.92	9.85	+39.00
3	12.796	10.52 9.86 11.06 9.56	9.86 9.89 10.50 9.10	10.07	+38.00
6	12.756	14.67 12.93 13.69 15.67	13.16 12.33 14.56 12.47	13.67	-28.00
8	12.682	7.38 6.65 6.98 9.32	9.52 9.38 10.68 8.90	8.32	-46.00
9	12.749	8.15 7.72 6.79 7.74	8.57 7.68 8.17 8.36	7.92	-49.00

Table 2.3: Zeta Potential of Titania powder

PH of the Solution	Position of the wall (cm)	Time for particle to cross 4 grids (sec)		Average time (sec)	Zeta potential (mV)
		When electric field is applied in the left direction	When the electric field is applied in the right direction		
2	12.760	9.96 9.49 9.89 10.28	10.43 9.66 11.13 10.79	10.2	38
3	12.758	9.51 9.34 9.16 9.67	9.93 9.32 9.86 9.77	9.72	40
6	12.656	19.70 16.32 16.88 16.30	21.72 21.58 18.06 17.45	18.50	21
8	12.646	10.37 11.76 11.21 10.92	12.57 9.40 10.83 11.00	11.007	-50
9	12.696	8.57 8.12 7.68 7.07	8.18 7.94 6.98 7.55	7.73	-35

2.1.1.4 X-RAY DIFFRACTION

The X-ray diffraction patterns were recorded using a Richiefert (ISO Debyeflex 2002D) diffractometer employing a filtered CuK_{α} radiation (λ=1.54 Å).

The X-ray diffraction plots (Intensity Vs. 2θ) of the powders were taken between 25°–80° in 2θ range .All the XRD patterns were recorded at room temperature. The conditions of the operation were as follows:

Scanning speed =1.2 ° per minute in 2θ

Chart speed =33 mm per minute

Time constant =3 sec

Counts per min =20 K

Operating point =(20 mA, 30kV)

The 2θ values corresponding to the appearance of peaks were noted from the diffraction patterns. The interplanar spacing could be calculated using Bragg's law

$$n\lambda = 2d \sin\theta$$

where n = order of reflection

λ = wavelength of the radiation used

d = interplanar spacing

θ = diffraction angle

The calculated d values and corresponding lattice parameters provided the information of the structure of the powders.

2.1.2 SEPARATION OF PARTICLES OF DIFFERENT SIZES

In order to see the effect of particle size on mixing as received powders have been separated into fractions of different sizes using

Table 2.4: Calculated times for setling through fixed distance

Powders	Setling time (in minutes) for 5 mm height		
	Particle Size		
	2μm	5μm	10μm
TiO_2	129	20.01	5.10
ZrO_2	78	12.5	3.07

2.1.3.MIXING OF POWDERS

Mixtures of TiO_2 and ZrO_2 powders with different volume fractions were prepared. In most of the experiments, nearly equal volume fractions of the two powders were used. In a few experiments different volume fractions were used. The calculation of the two powders to get the desired volume fraction is illustrated in Appendix I. The weighed amounts of TiO_2 and ZrO_2 powders as calculated were mixed in the following different ways-

(a) Dry mixing

(b) Mixing of aqueous suspension of powders at different pH.

2.1.3.1 DRY MIXING

The weighed amounts of TiO_2 and ZrO_2 powders were taken in a mortar and mixed for 15 minutes with the help of a spatula.

2.1.3.2 MIXING OF AQUEOUS SUSPENSIONS OF POWDERS

Different volume fractions of powders was mixed in aqueous suspensions at different pH combinations.

(i) Mixing of suspension of powders prepared at pH far from

sedimentation technique.

SEDIMENTATION TECHNIQUE

A spherical particle of density ρ_s and diameter a, released in a viscous fluid of density ρ_L and viscosity η will momentarily accelerate and then fall at a constant terminal velocity v. The terminal velocity is related to the particle diameter according to the Stoke's equation as[19]:

$$v = \frac{a^2(\rho_s - \rho_l)g}{18\eta}$$

where g is the acceleration due to gravity. The time t for settling through a height H is

$$t = \frac{18H\eta}{a^2(\rho_s - \rho_l)g}$$

Hence larger the particle diameter, lesser is the settling time. The sub micron particles can take several days to settle out. In this case the settling time can be reduced by centrifuging

$$t = \frac{18\eta \ln(r_t / r_0)}{a^2(\rho_s - \rho_l)w^2}$$

where w is the angular velocity of the centrifuge and r_0 and r_t are the radial positions of the particle before and after centrifuging.

PROCEDURE ADOPTED

We have separated particles of TiO_2 and ZrO_2 in fractions with the following size ranges (i) <2μm (ii) 2 to 5 μm (iii) 5 to 10 μm (iv) >10μm . First the powders were dispersed at pH9 (obtained by using NH_4OH in deionized water) and allowed to settle .The time for settling for these fraction of sizes are shown in table 2.4.

(ii) Mixing of suspension of powders when one is prepared at IEP.

MIXING PROCEDURE: WHEN SUSPENSIONS OF BOTH ARE FAR FROM IEP

Powders of TiO_2 and ZrO_2 were taken in 100 ml of aqueous solution having pH 9(prepared with the help of NH_4OH in distilled water) separately, stirred with the help of magnetic stirrer for around 15 minutes and then both the suspension were dispersed separately with the help of ultrasonic dismembered. Now the suspensions were mixed, stirred followed by ultrasonication. Now mixture is dried on hot plate with a constant stirring.

MIXING PROCEDURE, WHEN ONE OF THE SUSPENSION IS PREPARED AT IEP:

The suspension of powder prepared at isoelectric point was stirred for 15 minutes (not ultrasonicated) was mixed with the suspension of the powder prepared at pH far from IEP (stirred and ultrasonicated for 5 minutes). These suspensions were mixed and stirred again, ultrasonicated and dried on hot plate with constant stirring.

The dried mixed powders, pure TiO_2 and ZrO_2 powder were firmly pressed under 20 kN load of hydraulic press for 2 minutes with the help of die of diameter 12 mm, on releasing the load, we get the pellets. Now these pellets were loaded on the sample holder of Raman instrument separately for investigation.

2.2 EXPERIMENTAL SET UP

The successful application of spectroscopic methods requires an understanding of instrumentation. Considerable attention to the experimental details is therefore necessary. In Raman scattering very low intensity of scattering light is collected in the vicinity of relatively high intensity laser wavelength. One needs a highly sensitive spectroscopic system combined with very high discrimination i.e. the ability to see one feature and ignore another close to it in wavelength. With the advent of lasers, the method of recording spectra has been standardized to use a laser source , an efficient system for collecting the scattered light and a scanning multiple monochromator monitored by a high performance detector . Further Raman microprobe serves to focus the laser through the microscope objective to a small part of the sample and to collect the back scattered light .In this part we discuss the experimental aspect of the individual component used in Raman measurements.

2.2.1 EXCITATION SOURCE

A. Ar^+ ION LASER

An argon ion laser is an important and powerful excitation source fore light scattering .It can provide several discrete lines .The most important of these lines are centered at 488 nm and 514.5 nm .It can be operated in the single –line or multiple mode with an output of 5 watt. In the present experiment, a Spectra Physics Model – 165 Ar^+ ion laser consisting of laser head and Model 265 exciter is used. With a start boost circuit (by 7 kv pulse), the exciter generates an initial discharge in the plasma tube. The plasma tube in argon ion laser is made up of beryllium.

B. THE OPTICAL CAVITY CONSTRUCTION

The schematic of an argon ion laser is shown in Fig (2.1)

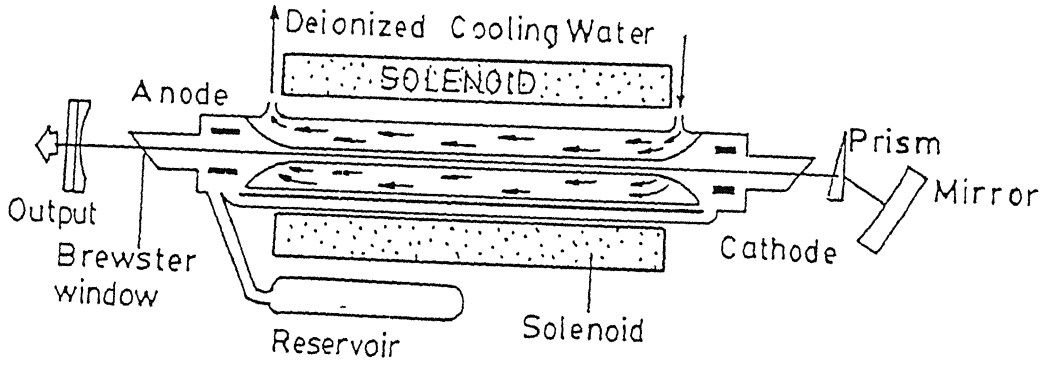

Fig (2.1) : Schematics of plasma tube Ar^+ laser and its cooling

The plasma tube containing argon gas is placed inside an optical resonator formed by a long radius flat reflector at the output and an assembly consisting of a prism and a mirror at the rear end. This rear optics can be tilted to provide maximum gain to a particular wavelength of lasing transitions. Both ends of the plasma tube are terminated by a fused Silica Brewster's angle window to get the plane polarized laser output and to minimize the cavity loses.

C. MAGNETIC HOUSING

The plasma tube is surrounded by a solenoid, which generates the magnetic field between 500 – 1000 Gauss. These magnetic field forces free electrons towards the center of the plasma tube bore, thereby increasing the probability of a pumping collision and population inversion. The magnetic field also causes Zeeman splitting, which elliptically polarizes the output resulting in partial loss at the polarization sensitive plasma tube windows. Susceptibility of the Zeeman effect varies from line to line and each line has an optimum magnetic field strength.

D. PLASMA EMISSION FROM LASERS

Although predominant output lies at one wavelength, it is accompanied by uncollimated radiations arising from the source discharge inside the laser. For Raman work, these uncollimated radiations must be avoided. Model 1450 tunable excitation filters are used to reject plasma emissions before the laser light is focused onto the sample .The laser mate Fig (2.2) consists of a grating that spectrally disperses incoming laser light, a beam

expander to increase the size of the spot on the grating a focusing mirror to direct the dispersed light through a fixed exit slit and a lens to collimate the light when passes through the exit slit. The plasma lines and adjacent lines are blocked by the slit body.

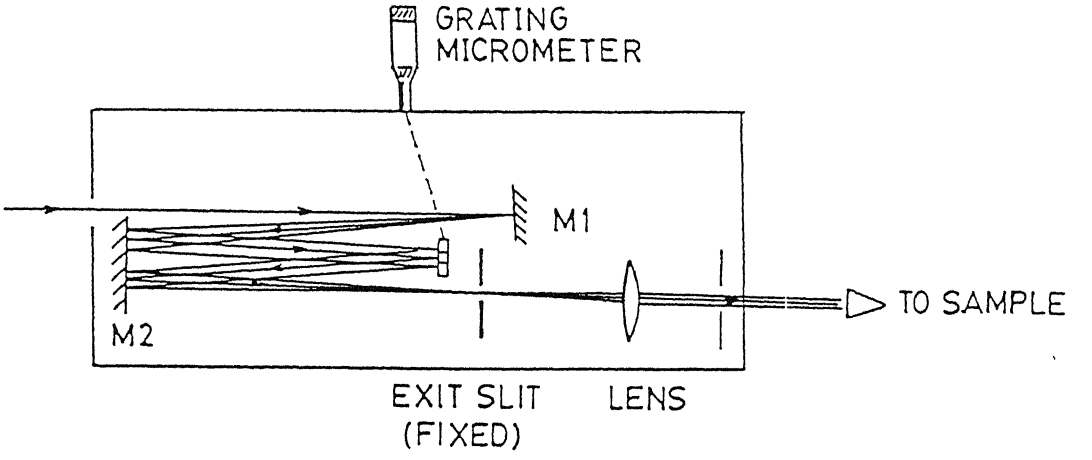

Fig (2.2) : Optical diagram of Tunable excitation filter/lasermate

E. COOLING SYSTEM FOR ARGON ION LASER

Argon ion laser requires cooling for the exciter and the plasma tube .The Neslab Chiller plants have been used for the cooling .The chiller plant mainly consists of a reservoir, temperature controller, recirculating pump and refrigeration unit. These chiller plants provide continuous flow of deionized water and constant temperature and pressure. Neslab HX-500 chiller plant has a maximum capacity of 15.7 kW and is used to cool the plasma tube and the exciter electronics of 5 watt Argon ion laser

F. LASER STABILITY

They design of resonator is very much crucial for the stability of oscillation of frequency. Small changes in the length of cavity cause corresponding changes in the resonant frequency. The length of the cavity changes due to the change in temperature, as,

$$\Delta L = L\alpha\Delta T$$

where L is the length of the cavity is the thermal expansion coefficient and t is the variation in the temperature. The ideal material is one,. Which has low thermal expansion coefficient. The Graphite composite used in the model 2030 resonator has the lowest thermal expansion coefficient of any currently used structural material.

2.2.2 FOCUSING OPTICS

The optical components used for focusing the laser beam are used in a configuration that helps to minimize the intensity loss from the incident as well as the scattered radiation from the sample. The selection of these optical components is based on a detailed estimation of several optical parameters, in particular focal length of the combination of collecting lenses, the dispersivity of the prism, mirror reflectivity etc, with a view to obtain maximum efficiency. As shown in Fig (2.3), the output of the laser source is allowed to fall on a beam steerer which comprises of two vertically displaced, highly reflecting mirrors (average reflectance ~ 92 %) placed at 90° to each and 45° to the vertical axis, which results in a vertical displacement of the beam to the level of the

entry slit of the monochromator. The beam is now directed towards a right-angled prism which has a surface flatness of ~95%. This prism reflects the beam at an angle of 90° through a small mirror surface allows the beam to fall on the sample. This scattered beam from the sample is imaged on the entrance slit of the monochromator using a collecting and focusing lens. Incase of liquid samples, a spherical mirror is placed behind the sample so as to minimize the losses of the scattered radiation from the sample.

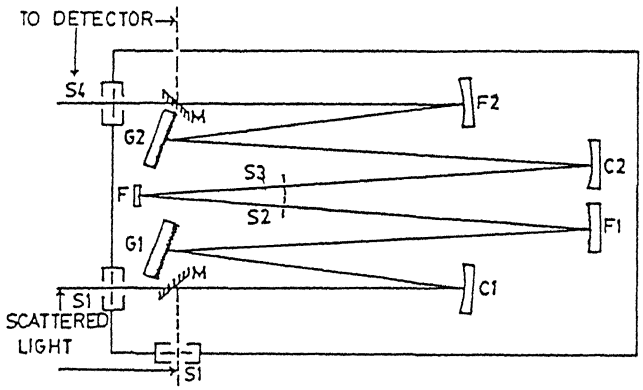

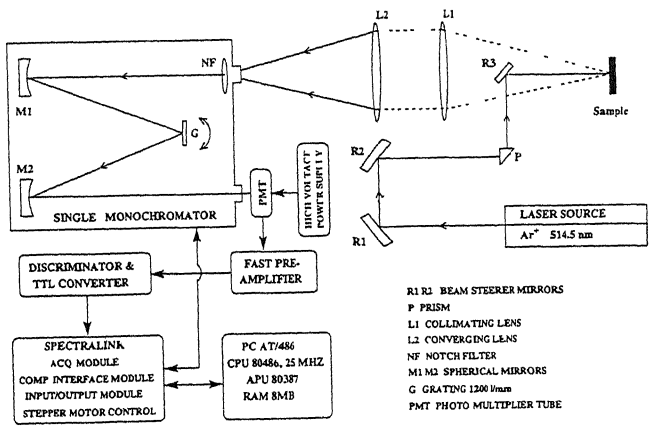

Fig (2.3) : Schematic diagram of the focusing optics

2.2.3 THE MONOCHROMATOR

Raman monochromators are invariably composed of two or more systems operating in sequence. The Spex 1877E triplemate is a spectrograph specially tailored to provide the low-stray light and flat undistorted focal plane, ideal for sensitive work with optical multichannel detectors. The schematic optical diagram of Spex 1877E triplemate has shown in Fig (2.4)

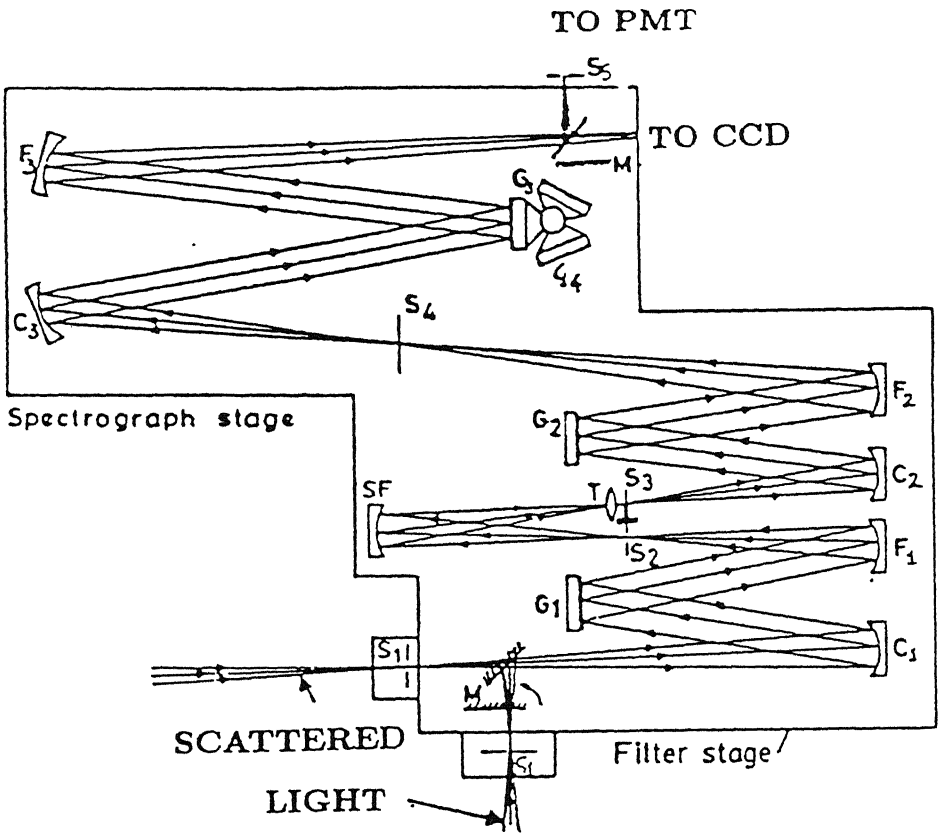

Fig (2.4) : Schematic optical diagram of Spex 1877E triplemate

2.2.4 CCD DETECTOR

The charge coupled device (CCD) detector has been demonstrated to show unmatched sensitivity in Raman Spectroscopy. The CCd is an

optical array detector, the operation of which is based on the accumulation of photo generated charge carriers. The collected charge is transported sequentially to a single charge sensor and then recorded. The peak efficiency of this device is centered in the red/ near infrared spectral regions, making the CCD an ideal for Raman spectroscopic application. Along the focal plane of the spectrometer the Spex spectrum CCD array is mounted in Liq. Nitrogen. Dewar assembly, which cools the array for very low thermal noise loss. An interface unit connects the Dewar mounted CCD to the computer.

2.2.5 SOFTWARE

A. DATA ACQUISITION

The data acquisition and parameter control is carried out through the dM 3000 Raman software. This software is a completely integrated series of programs and spectral routines for the acquisition and treatment of spectroscopic data. It has been written to work with MS DOS versions 5.0, 6.0 or higher .The software allows for a flexible use of most standard models of acquisition and helps in creation, storage and modification of acquisition routines.

B. DATA ANALYSIS

The analysis of the experimental data obtained from the Raman measurement is carried out using perfect commercial non- linear curve fitting package. This package provides data editing, conversion of units, deconvolution of the peaks, calculation of peak areas as well as the line width and back ground removal

2.2.6 CALIBRATION

Diamond sample is used for calibration of the instrument usually. It is one of the few materials which has revolutionized many a technology e.g. high pressure physics, thin films, electronics etc .The spectrum of the diamond type 2 with 2mwatt laser power is shown in the Fig (2.5) .It is clear that a very sharp Raman transition is obtained which is found to be centered at 1333.1 cm^{-1} .

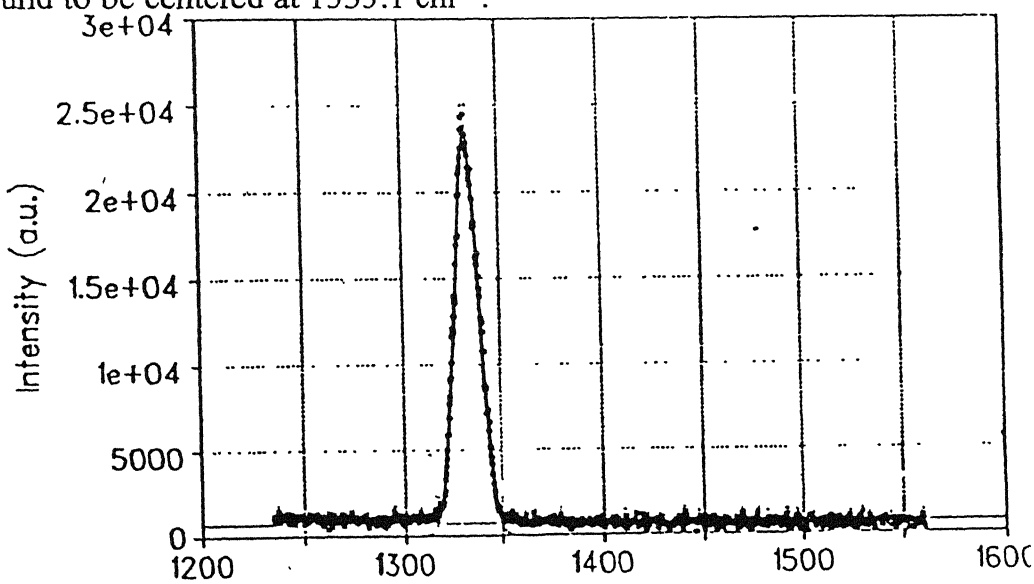

Fig (2.5) The Raman spectra of diamond

2.2.7 CONDITIONS TO RECORD RAMAN SPECTRA

In the present work we have used the following conditions in order to record the Raman spectra of the samples

Laser power = 300 mW

Wavelength used = 514.5 nm

Filter position = 500 nm

Exposure time = 1 sec

Spot size = 2 μm and 10 μm

CHAPTER 3
RESULTS AND DISCUSSIONS

This chapter deals with the experimental results. The results on the characterization of powders are described first followed by the main results on mixing of the powders by Raman spectroscopy.

3.1 POWDER CHARACTERIZATION RESULTS

3.1.1 PARTICLE SIZE

The output from the particle size analyzer for the TiO_2, ZrO_2 (MEL) and ZrO_2 (TOSOH) are shown in Fig (3.1a-c) respectively. As can be seen the TiO_2 powder is nearly monodispersed with average size (50%) of about 0.4 μm .The ZrO_2 and the rest have a particle size of about 7-8 μm. ZrO_2 (TOSOH) has a broad distribution with two broad overlapping peaks at about 0.7 and 4 μm. The ZrO_2(MEL) has bimodal distribution plot; it has average particle size of about 0.4 μm and near about 20 % of the powder has a particle size of 5μm.

3.1.2 PHASES

The X-ray diffraction patterns of TiO_2, ZrO_2 (MEL) and ZrO_2 (TOSOH) are shown in the figures (3.2a-3.2c) respectively. The 2θ values and relative intensities of various peaks together with their indices assigned are given in tables 3.1 and 3.2. The results clearly reveal that TiO_2 has anatase structure while ZrO_2 (MEL) and ZrO_2 (TOSOH) both have monoclinic structure.

Table 3.1: 2θ values and intensities of various peaks observed in XRD of TiO_2

2θ Degrees	Relative Intensity	(hkl)
25.3	100	101
36.9	10	103
37.8	20	004
38.6	10	112
48.0	35	200
53.9	20	105
55.2	20	211
62.0	4	213
62.7	14	204
68.8	6	116
70.3	6	220

Table 3.2: 2θ values and intensities of various peaks observed in XRD of ZrO_2 (MEL)

2θ Degrees	Relative Intensities	(hkl)
28.4	100	$\bar{1}11$
31.6	64	111
34.2	22	022
35.3	14	200
38.5	5	021
40.7	12	$\bar{2}11$
41.2	6	102
44.9	7	112
45.5	6	211
49.2	16	022
50.1	18	$\bar{2}20$
54.0	11	200
55.4	12	013

3.1.3 PARTICLE SURFACE AREA

The surface area of the powders (as received) has been measured using single point BET method. The specific area of MEL ZrO_2 and TiO_2 are determined to be 4.57 and 11.31 m^2/gm respectively.

FRITSCH PARTICLE SIZER A N A L Y S E T T E 22

63 | 12-17-1999 | 16 18 | FA FRITSCH | UserID LAB/22 | SerNo SN3165 |

TiO2-Aldrich--99 9%

Finer

Measuring Range	0 10 [µm] -	31 66 [µm]		Pump	90 [rpm]
Resolution	62 Channels	(9 mm / 12 mm)		Stirrer	90 [rpm]
Absorption	12 00 [%]			Ultrasonic	90

Measurement Duration C:\A22WIN\FRITSCH\PARTICL1.FPS

98 87 % <	1 00 µm	100 00 % <	2 00 µm	100 00 % <	3 00 µm
100 00 % <	4 00 µm	100 00 % <	5 00 µm	100 00 % <	6 00 µm
100 00 % <	7 00 µm	100 00 % <	8 00 µm	100 00 % <	9 00 µm
100 00 % <	10 00 µm	100 00 % <	20 00 µm	100 00 % <	30 00 µm
****** % <	40 00 µm	****** % <	50.00 µm	****** % <	60 00 µm
****** % <	70 00 µm	****** % <	80 00 µm	****** % <	90 00 µm
****** % <	100.00µm	****** % <	200 00µm	****** % <	300 00µm
****** % <	400.00µm	****** % <	500 00µm	****** % <	600.00µm
****** % <	700 00µm	****** % <	800 00µm	****** % <	900 00µm
****** % <	1000 00µm				

Interpolation Values .. C:\A22WIN\FRITSCH\PERCENTS.FPV

95 00 % >	0 18 µm	90.00 % >	0 21 µm	85 00 % >	0 24 µm
80 00 % >	0 26 µm	75 00 % >	0 29 µm	70.00 % >	0 32 µm
65 00 % >	0 34 µm	60 00 % >	0 37 µm	55 00 % >	0 39 µm
50 00 % >	0 42 µm	45 00 % >	0 44 µm	40 00 % >	0 47 µm
35 00 % >	0 50 µm	30 00 % >	0 53 µm	25 00 % >	0 57 µm
20 00 % >	0 61 µm	15 00 % >	0 66 µm	10 00 % >	0 72 µm
5 00 % >	0 83 µm	1 00 % >	1 01 µm		

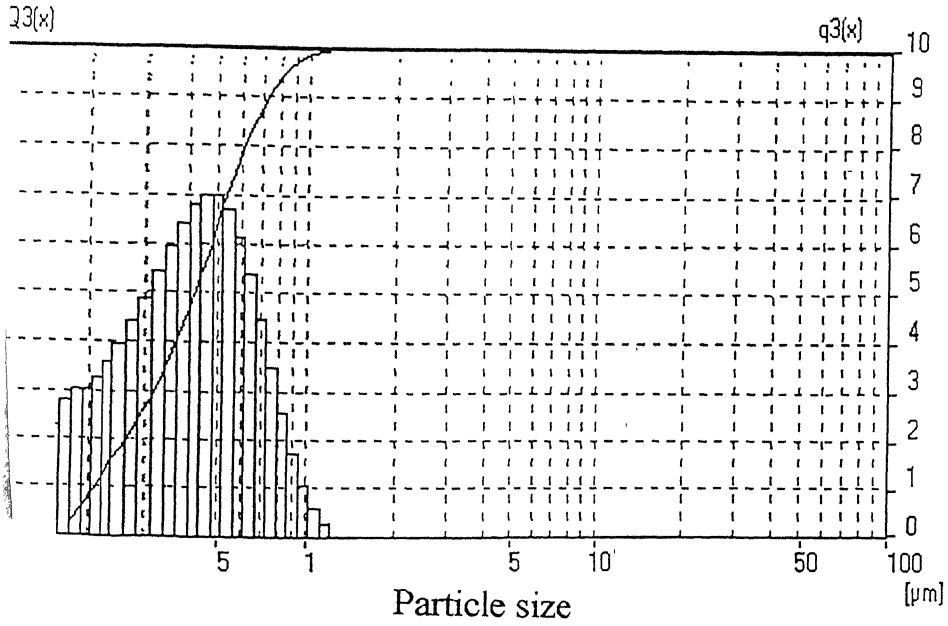

Fig(3.1a) : Particle size plot of TiO_2 powder

FRITSCH PARTICLE SIZER ANALYSETTE 22

Here you can place a user defined message

63	09-06-1999	16 05	FA FRITSCH	UserID LAB/22	SerNo SN3165

ZrO2 Magnesio Ltd

Measuring Range	0 10 [µm] - 29 02 [µm]	Pump	90 [rpm]
Resolution	62 Channels (9 mm / 11 mm)	Stirrer	90 [rpm]
Absorption	10 00 [%]	Ultrasonic	90
Measurement Duration	20 [Scans]		

Interpolation Values C \A22WIN\FRITSCH\PARTICL1 FPS

Specified Cumulation selected		81 20 % <	2 00 µm	81 39 % <	3 00 µm
[illegible]		83 62 % <	5 00 µm	85 67 % <	6 00 µm
89 38 % <	7.00 µm	93 20 % <	8 00 µm	95 91 % <	9 00 µm
97 67 % <	10 00 µm	99 80 % <	20.00 µm	****** % <	30 00 µm
****** % <	40 00 µm	****** % <	50 00 µm	****** % <	60 00 µm
****** % <	70 00 µm	****** % <	80.00 µm	****** % <	90 00 µm
****** % <	100 00µm	****** % <	200 00µm	****** % <	300 00µm
****** % <	400 00µm	****** % <	500 00µm	****** % <	600 00µm
****** % <	700 00µm	****** % <	800 00µm	****** % <	900 00µm
****** % <	1000 00µm				

Interpolation Values C \A22WIN\FRITSCH\PERCENTS FPV

95 00 % >	0.18 µm	90.00 % >	0 21 µm	85.00 % >	0 23 µm
80 00 % >	0 26 µm	75 00 % >	0 28 µm	70.00 % >	0 30 µm
65 00 % >	0.32 µm	60 00 % >	0 35 µm	55.00 % >	0 37 µm
50 00 % >	0 39 µm	45 00 % >	0 42 µm	40 00 % >	0 45 µm
35 00 % >	0 48 µm	30 00 % >	0 51 µm	25.00 % >	0 57 µm
20 00 % >	0 69 µm	15 00 % >	5 77 µm	10 00 % >	7 15 µm
5 00 % >	8 60 µm	1 00 % >	11.53 µm		

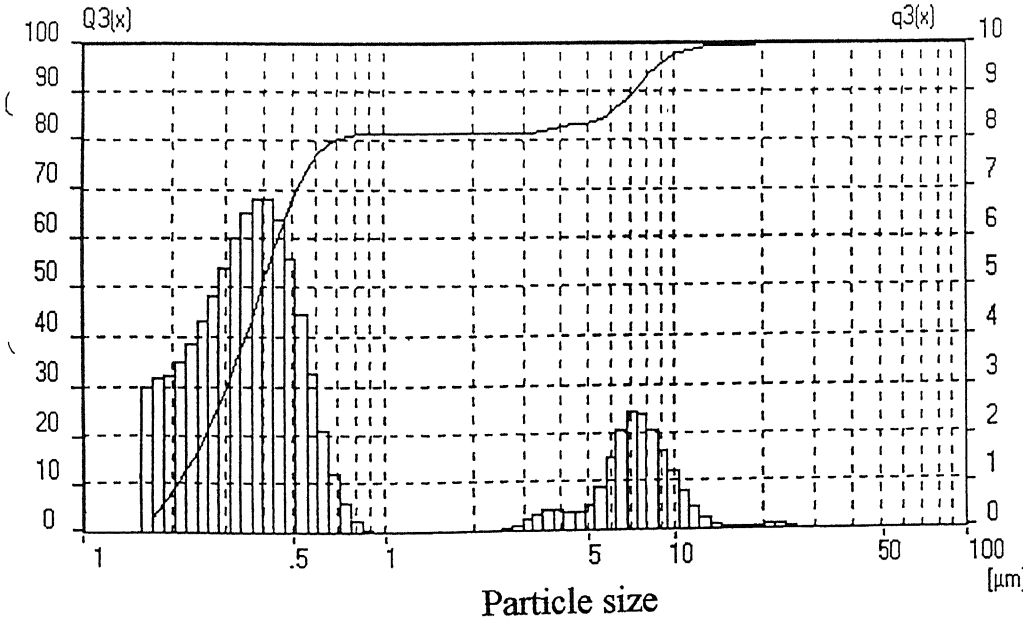

Fig(3.1b) : Particle size plot of ZrO_2 (MEL) powder

FRITSCH PARTICLE SIZER A N A L Y S E T T E 2 2

Here you can place a user defined message TOSOH ZrO2

65	09-20-1999	10 58	FA FRITSCH	UserID LAB/22	SerNo SN3165

TOSOH

~~TOS~~AB-ZrO2

Measuring Range	0 10 [µm] - 50 12 [µm]	Pump	90 [rpm]
Resolution	62 Channels (9 mm / 19 mm)	Stirrer	90 [rpm]
Absorption	19 00 [%]	Ultrasonic	90
Measurement Duration	20 [Scans]		

Interpolation Values C \A22WIN\FRITSCH\PARTICL1 FPS

Model Independant

Fraunhofer Calculation selected

44 06 % <	1 00 µm	64 29 % <	2 00 µm	75 22 % <	3 00 µm
84 14 % <	4 00 µm	91 22 % <	5 00 µm	95 96 % <	6 00 µm
98 57 % <	7 00 µm	99 68 % <	8 00 µm	99 99 % <	9 00 µm
100 00 % <	10 00 µm	100 00 % <	20 00 µm	100 00 % <	30 00 µm
100 00 % <	40 00 µm	****** % <	50 00 µm	****** % <	60 00 µm
****** % <	70 00 µm	****** % <	80 00 µm	****** % <	90 00 µm
****** % <	100 00µm	****** % <	200 00µm	****** % <	300 00µm
****** % <	400 00µm	****** % <	500 00µm	****** % <	600 00µm
****** % <	700 00µm	****** % <	800 00µm	****** % <	900 00µm
****** % <	1000 00µm				

Interpolation Values C.\A22WIN\FRITSCH\PERCENTS FPV

95 00 % >	0 26 µm	90 00 % >	0.35 µm	85 00 % >	0 43 µm
80 00 % >	0 50 µm	75.00 % >	0 58 µm	70 00 % >	0 67 µm
65.00 % >	0 77 µm	60.00 % >	0 89 µm	55 00 % >	1 03 µm
50 00 % >	1 20 µm	45 00 % >	1 42 µm	40 00 % >	1 70 µm
35 00 % >	2 05 µm	30 00 % >	2 49 µm	25 00 % >	2 98 µm
20.00 % >	3 52 µm	15 00 % >	4 11 µm	10 00 % >	4 80 µm
5 00 % >	5 73 µm	1 00 % >	7 31 µm		

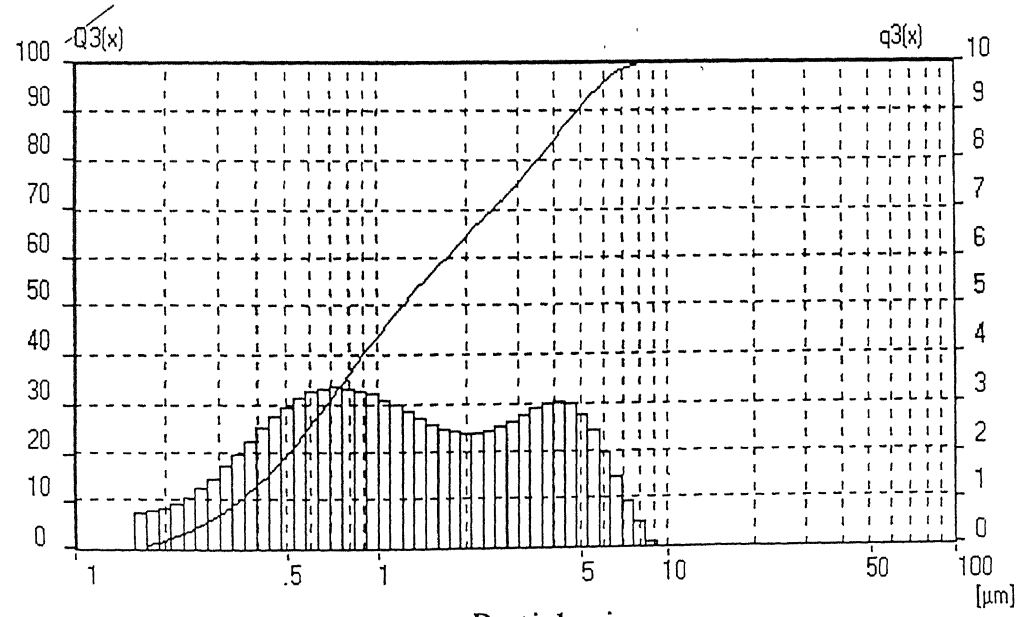

Particle size

Fig(3.1c) : Particle size plot of ZrO_2 (TOSOH) powder

Fig(3.2a): X-ray diffraction pattern of TiO_2 powder

Fig(3.2b) : X-ray diffraction pattern of ZrO_2 (MEL) powder

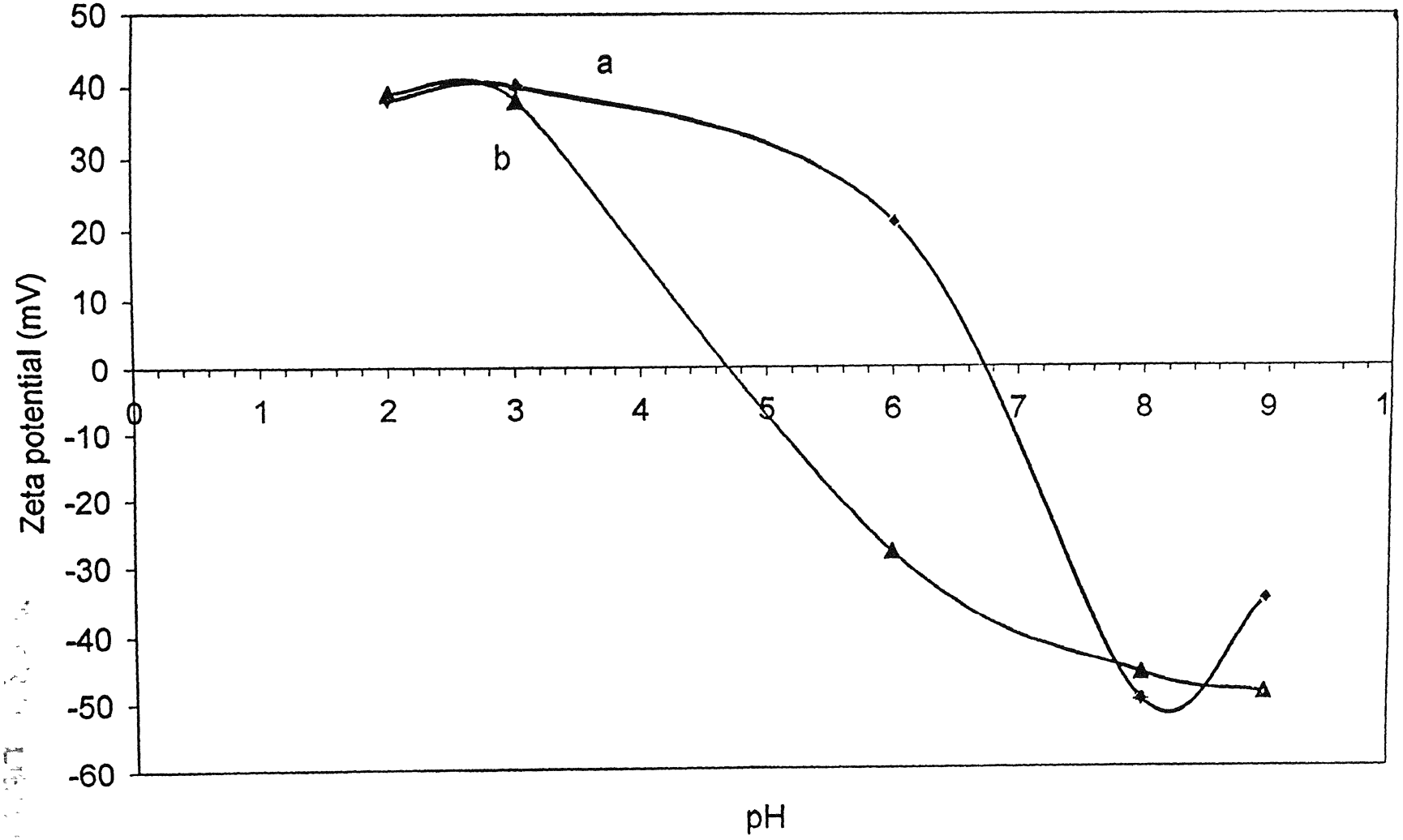

Fig(3.3) :Zeta Potential Vs pH (a) ZrO_2 (b) TiO_2

3.2 RAMAN SPECTRA FROM PURE POWDERS

3.2.1 RAMAN SPECTRA FROM TIO_2

Raman spectra of pure TiO_2 has been obtained at the conditions described earlier .The computer interfacing (with the Raman instrument) which has the dM3000R software provides SPT file. This file is converted into text file using ASCII output file commands as given in Appendix II(b).

The Fig (3.3) and Fig (3.4) show the Raman spectra of pure TiO_2 at room temperature obtained using 2 μm beam size and after background removal respectively. Raman spectra of TiO_2 (anatase) powder is identical to that reported in the literature.[23] The frequencies of the Raman bands are observed at 637, 515 and 396 cm^{-1}. These bands are assigned to Eg, (A1g, B1g) and B1g modes respectively[23]. The frequency band at 515 cm^{-1} is basically a doublet.

3.2.2 RAMAN SPECTRA FROM ZIRCONIA

Fig (3.5) and Fig (3.6) show the Raman spectra of zirconia (MEL and TOSOH) at room temperature using 2 μm beam size before and after background removal respectively. These are matching well with the

reported spectra of pure zirconia in the literature.[21] It has 14 – 16 bands as predicted theoretically.[22] The bands of the spectrum are sharp and intense. The spectra were recorded at different spots on the same pellet as well as on different pellets and no variations in the spectra were observed. It should be noted that Raman intensity for zirconia is much less as compared to titania.

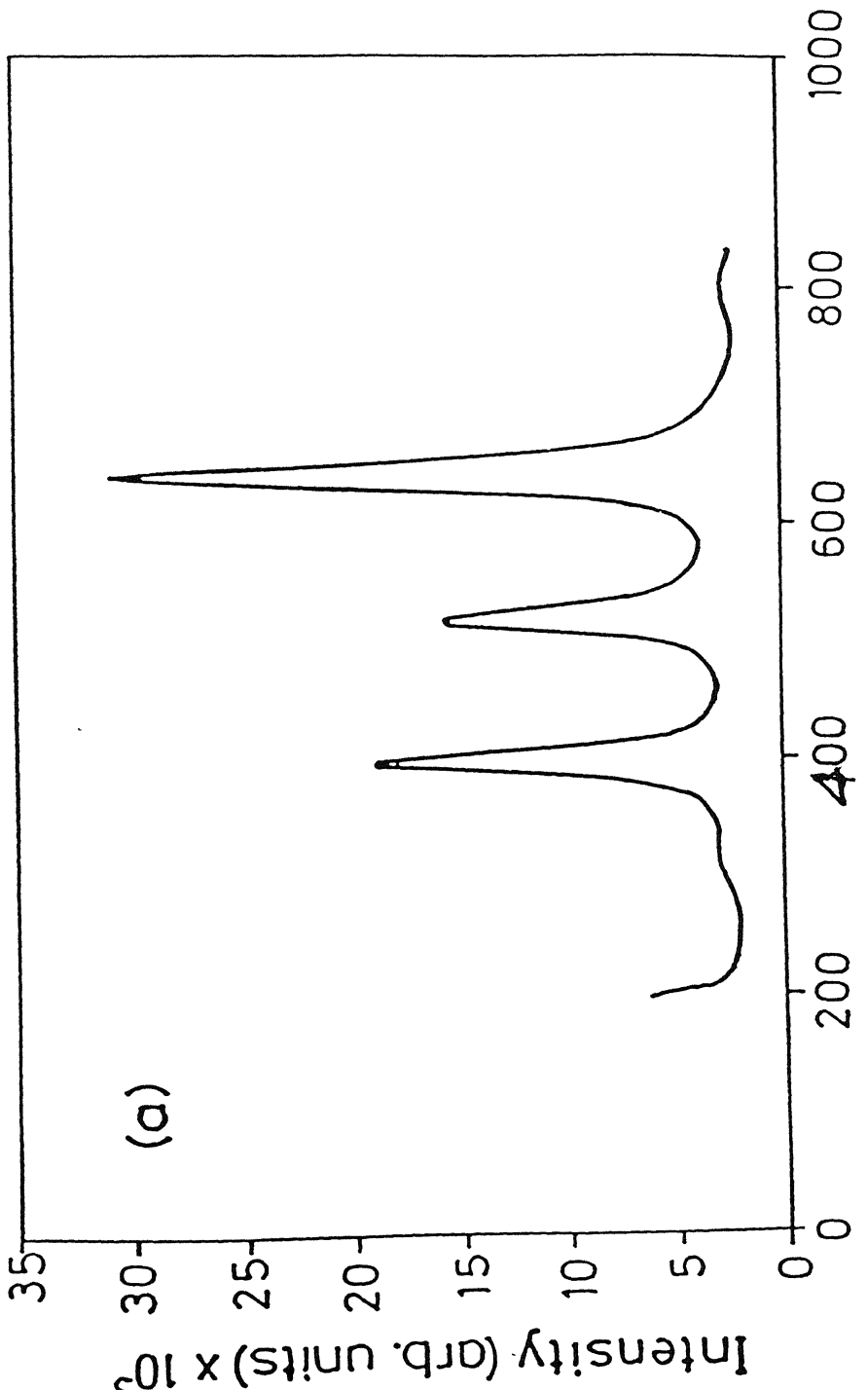

Fig(3.4): Raman Spectra of pure TiO_2

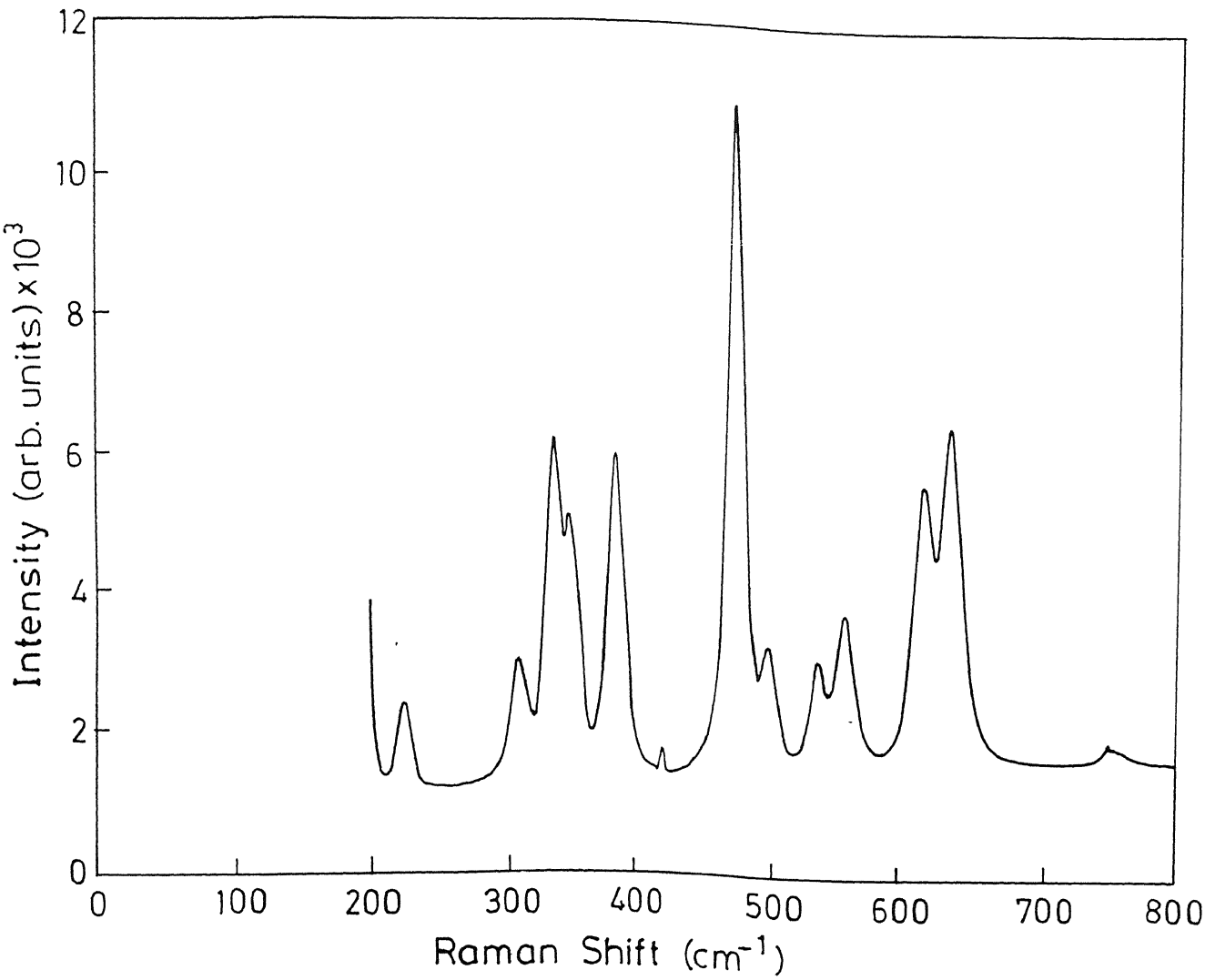

Fig(3.5): Raman spectra of pure ZrO_2 (MEL) as recorded

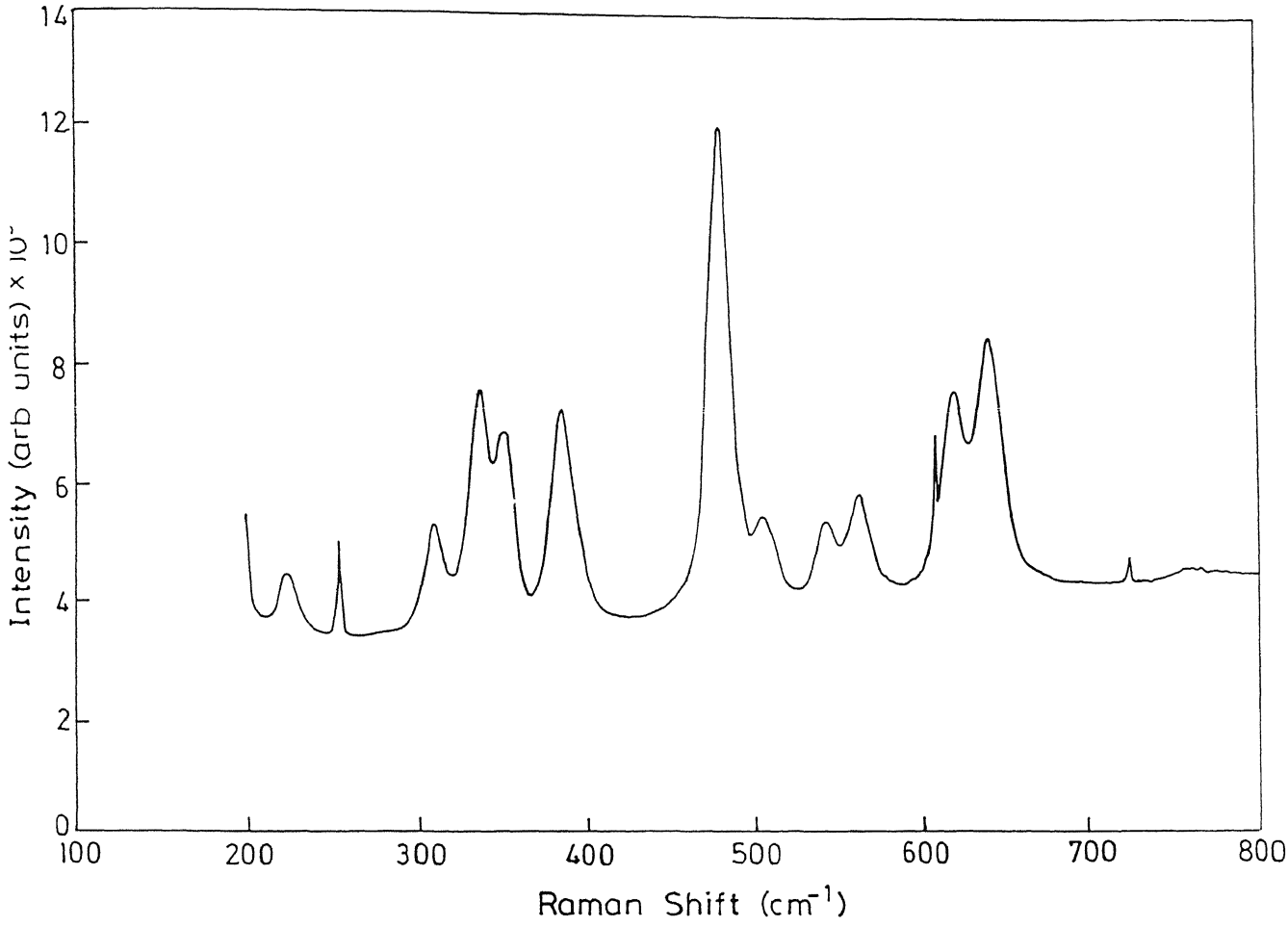

Fig(3 6) : Raman spectra of pure ZrO_2 (TOSOH) as recorded

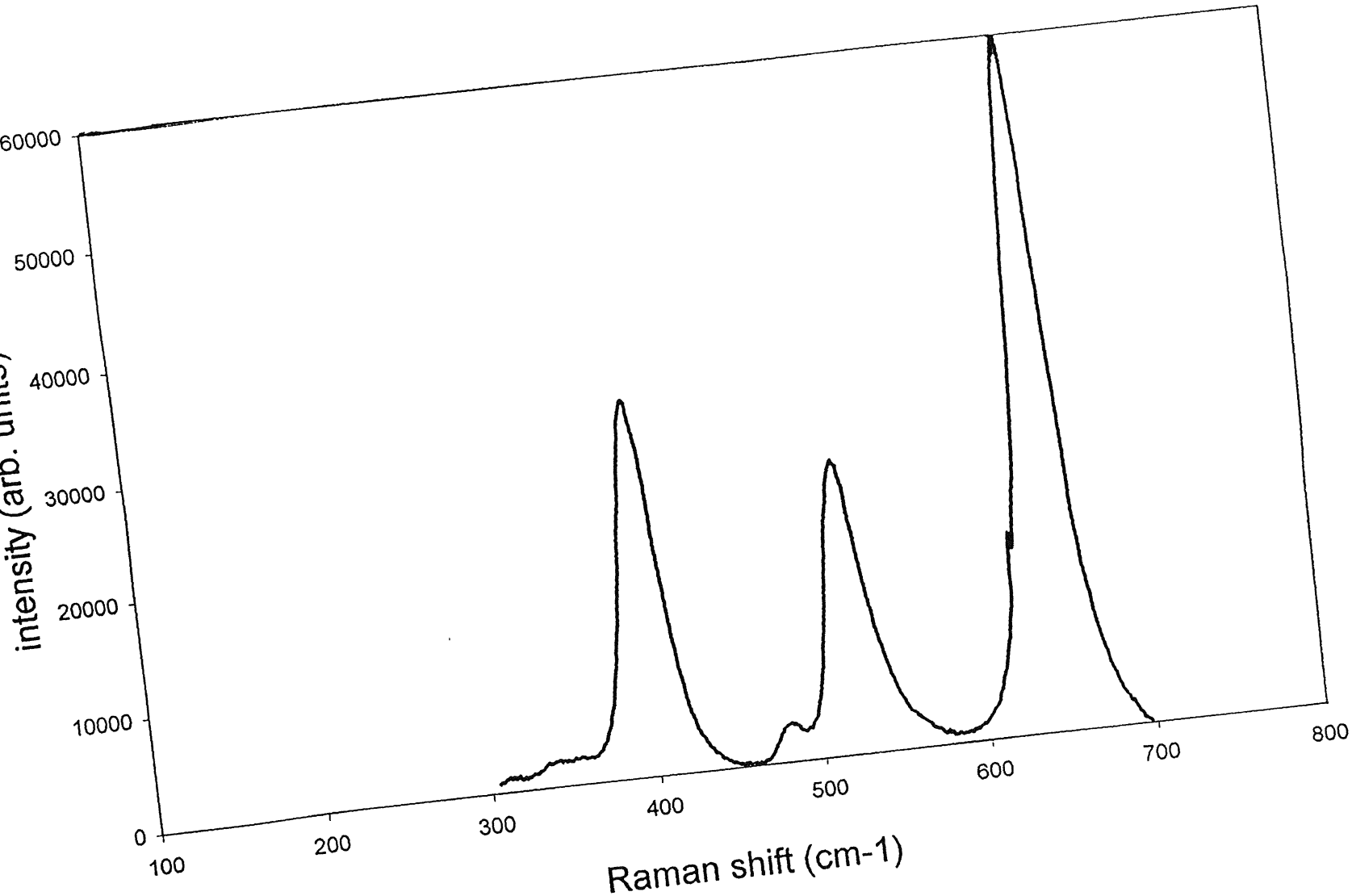

Fig(3.7): Raman spectra of dry mixed powder

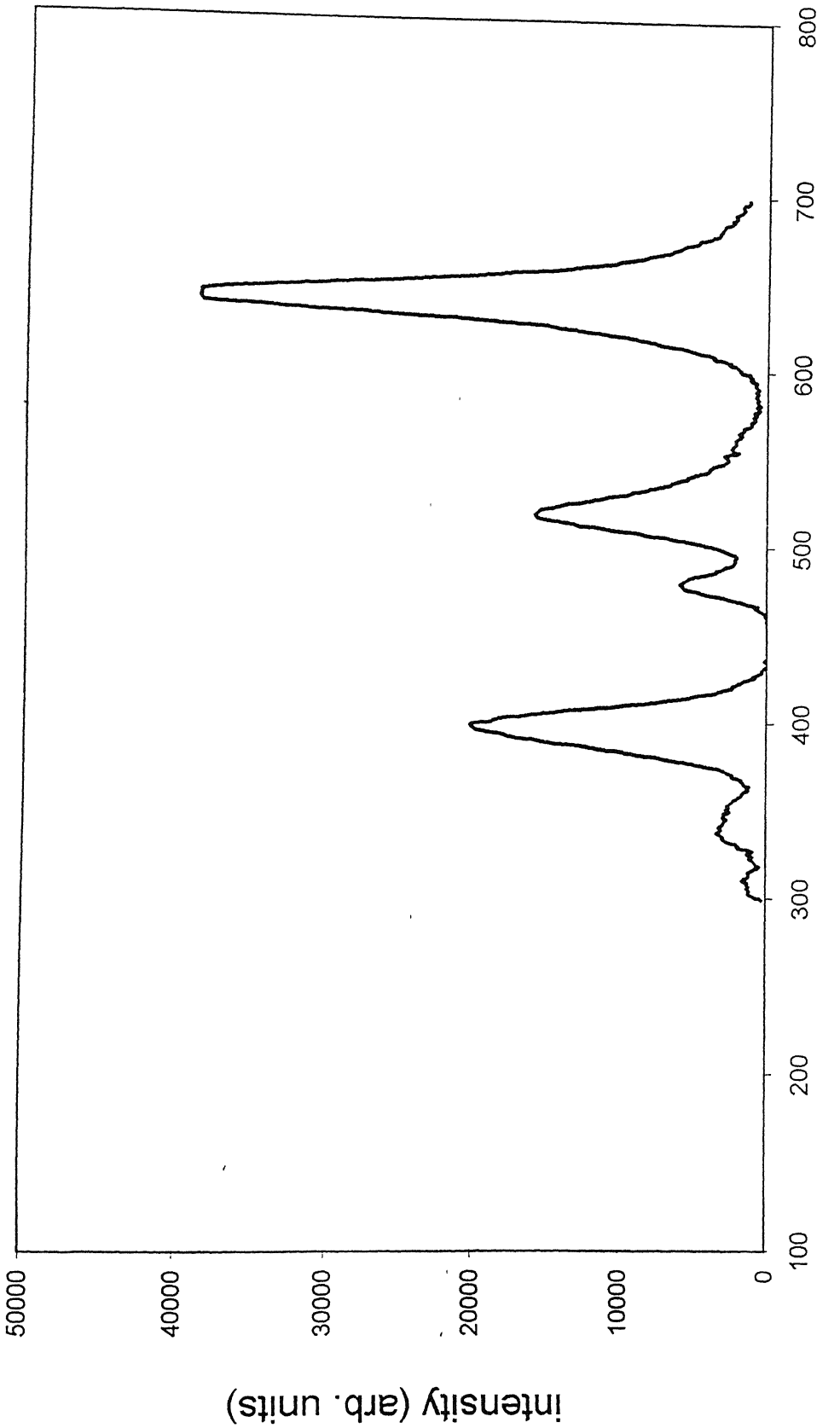

Fig(3.8). Raman spectra of powder mixed at pH 9:9

Fig(3.9): Raman spectra of experimental and fitted curve of the dry mixed powders

3.3 MIXTURES OF POWDERS

3.3.1 RAMAN SPECTRA FROM THE MIXTURES

The Raman spectra of the mixtures prepared under different conditions have been obtained under same conditions as for the pure powders. Fig (3.7) shows the Raman spectra of dry mixed powder and the powder mixed at pH 9:9 (ZrO_2: TiO_2) using 2μm beam size. The spectra show the peaks predominantly from titania. This is because the scattered intensity in titania is much stronger than from zirconia. A few peaks of high intensity in zirconia can also be seen.

3.3.2 ANALYSIS OF RAMAN SPECTRA FROM MIXTURES

The Raman spectra of the mixture have been fitted to a linear combination of the spectra from the pure powder (i.e. x TiO_2 + y ZrO_2). Fig (3.8) shows the experimental and fitted curves for the dry mixed powders. It is seen that a very good fit is obtained. The values of x and y are unique.

To a first approximation, the relative contributions of the two constituents of the mixed powder, namely TiO_2 and ZrO_2 to the Raman spectra of the mixture are proportional to their relative surface areas exposed to the laser beam. Assuming that the sample surface is flat, the value of x and y would be proportional to the area fraction of the TiO_2 and ZrO_2 surfaces. The area fraction thus determined are equal to the volume fractions of the two surface, [25] Thus by fitting the spectra from the mixture

of powders to a linear combination of the spectra from the pure powders, the volume fraction of TiO_2 and ZrO_2 are obtained. In the following discussion, the result have been presented in terms of volume fractions

3.4 EFFECT OF MIXING TECHNIQUE ON THE DEGREE OF MIXING

In this section, the results of the various experiments carried out to evaluate the degree of mixing using Raman spectroscopy are presented. A total of four sets of experiments were performed,

(i) Powders of TiO_2 and ZrO_2 (TOSOH) mixed by dry mixing and from suspensions of ZrO_2 and TiO_2 at pH 6:3, 6:6 and 3:3 respectively

(ii) Powders of TiO_2 and ZrO_2 (MEL) mixed by dry mixing and from suspensions of ZrO_2 and TiO_2 at pH 9:4, 9:9, 6:9 and 6:6 respectively

(iii) Powders of TiO_2 and ZrO_2 (MEL) mixed from suspensions of pH 9:9 with volume fraction of TiO_2, 0.25, 0.486 and 0.75 and

(iv) Powders of TiO_2 and ZrO_2 (MEL) of different particle sizes mixed at pH 9:9.

Two combinations of particle sizes were used. In the first one both the powders have the particle sizes more than 10 μm while in the second case both the powders have particle size less than 2 μm.

3.4.1 EXPERIMENTS OF SET I

This set of experiments was carried out on the mixtures prepared using TiO2 and ZrO2 (TOSOH) powders in nearly equal volume fractions (0.486:0.514). Table (3.3) gives the volume fractions of TiO_2 determined by Raman spectra of the mixtures prepared by different methods. Fig (3.9) shows a plot of the same data.

Table 3.3: Results of set 1: TiO_2 + ZrO_2 (TOSOH); actual volume fractions 0.486: 0.514; laser beam size = 2 μm

pH of suspension ZrO_2:TiO_2	Volume fraction TiO_2
(Dry mixing)	0.85, 0.66, 0.0, 0.36
6:3	0.80, 0.87, 0.87, 0.81
6:6	0.80, 0.76, 0.85, 0.89
3:3	0.69, 0.71, 0.66, 0.70

3.4.2 EXPERIMENTS OF SET II

In the second set of experiment, powders of titania and zirconia (MEL) were used. The two powders were mixed in nearly equal volume fractions (0.486:0.514). The results of this set are given in table 3.4 and plotted in fig (3.10).

Table 3.4: Results of set II: TiO_2 +ZrO_2 (MEL); actual volume fraction 0.486:0.514;

pH of suspension ZrO_2:TiO_2	Volume fraction TiO_2	
	Beam size 2μm	Beam size 10μm
(Dry mixing)	0.52, 0.67, 0.67, 0.5, 0.5, 0.0	0.4, 0.7, 0.26, 0.5, 0.64, 0.5
9:4	0.47, 0.58, 0.3, 0.54,	0.3, 0.46, 0.39, 0.31, 0.36, 0.25, 0.27, 0.38, 0.24
9:9	0.57, 0.60, 0.32, 0.56, 0.60	0.25, 0.25, 0.50, 0.50, 0.28, 0.41, 0.39, 0.43, 0.28, 0.42
6:9	0.46, 0.47, 0.49, 0.41	0.38, 0.44, 0.35, 0.29, 0.37, 0.50, 0.56, 0.48
6:6	0.48, 0.41, 0.34,	0.42, 0.48, 0.50, 0.47, 0.50, 0.39, 0.45, 0.42

3.4.3 EXPERIMENTS OF SET III

In this set of experiment, powders of titania and zirconia (MEL) were used. The two powders were mixed in different volume fractions. The results of this set are given in table 3.5 and plotted in fig (3.11).

Table 3.5: Results of set III: TiO_2 +ZrO_2 (MEL); mixed from suspensions at pH 9:9; laser beam size 10 μm.

Actual volume fraction of TiO2 in the mixture	Volume fraction of TiO2 determined from Raman spectroscopy
0.25	0.16, 0.17, 0.18, 0.21, 0.18, 0.19, 0.17, 0.15
0.50	0.25, 0.25, 0.50, 0.50, 0.28, 0.41, 0.39, 0.43, 0.28, 0.42
0.75	0.67, 0.65, 0.71, 0.69

3.4.4 EXPERIMENTS OF SET IV

In this set the powder mixtures having volume fraction TiO_2:ZrO_2::0.486:0.514 were prepared using powders having particle sizes either ≤ 2 μm or ≥ 10 μm. The original powders, which had wide size distributions were, separated into two fractions as described earlier. It was found that the fractionated ZrO_2 powders showed considerable amount of photoluminescence. Fig (3.13) shows the photoluminescence from ZrO_2 with particle size < 2 μm. Curve (a) is from the original powder while curves (b) and (c) are from the same spot after irradiating with the laser beam (quenching) for 15 minutes and 30 minutes respectively. It can be seen that there is a significant amount of photoluminescence whose intensity decreases on quenching.

Fig (3.13) shows the Raman spectra from ZrO_2 powder with particle size < 2 μm. Curves a, b, c and d are nearly featureless showing only a monotonic increase. This is the initial part of the PL observed in zirconia Fig (3.13). Also, the intensity profiles change with exposure time. Because of these reasons (overlapping PL) Raman peaks from the sample with particle size less than 2 μm could not be observed. The intensity of photoluminescence was much less in ZrO_2 powders with particle size $>$ 10 μm and so, on quenching, the Raman spectra could be observed distinctly. For the mixtures of zirconia powders with particle size > 10 μm, all the spectra for pure powder as well as for the mixtures were taken after 15 minutes of quenching. Also, as the TiO_2 powder did not show any photoluminescence, the data from the mixture with particle size > 10 μm could be analyzed as before. The experimentally determined volume

fractions of TiO_2 in this case vary between 0.27 and 0.68 as compared to the actual volume fraction of 0.486.

The actual values obtained from analysis from five different spots using 10 μm beam size were 0.27, 0.33, 0.31, 0.68 and 0.34.

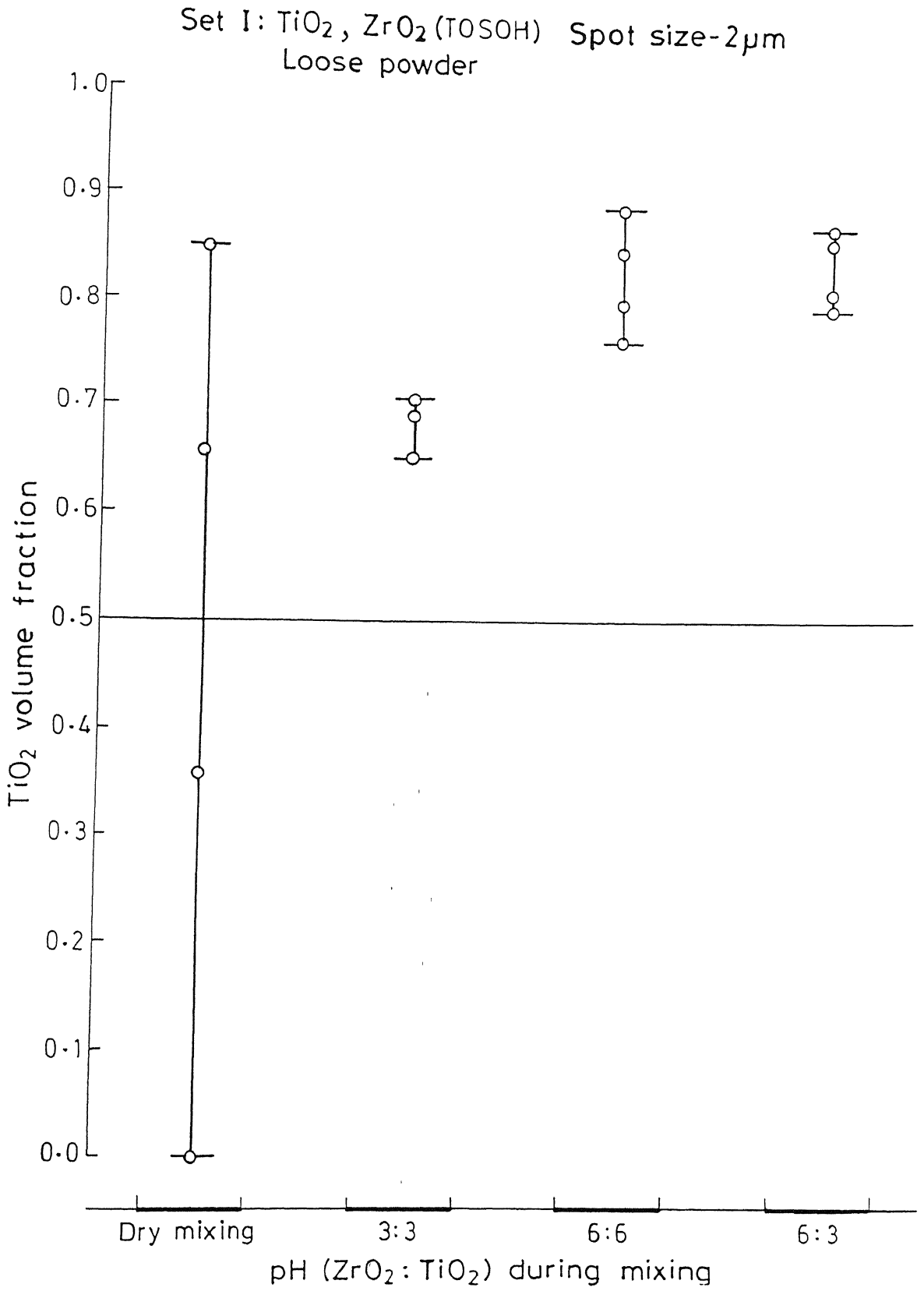

Fig (3.10): The plot showing volume fraction of Tio_2 at different mixing methods set-I

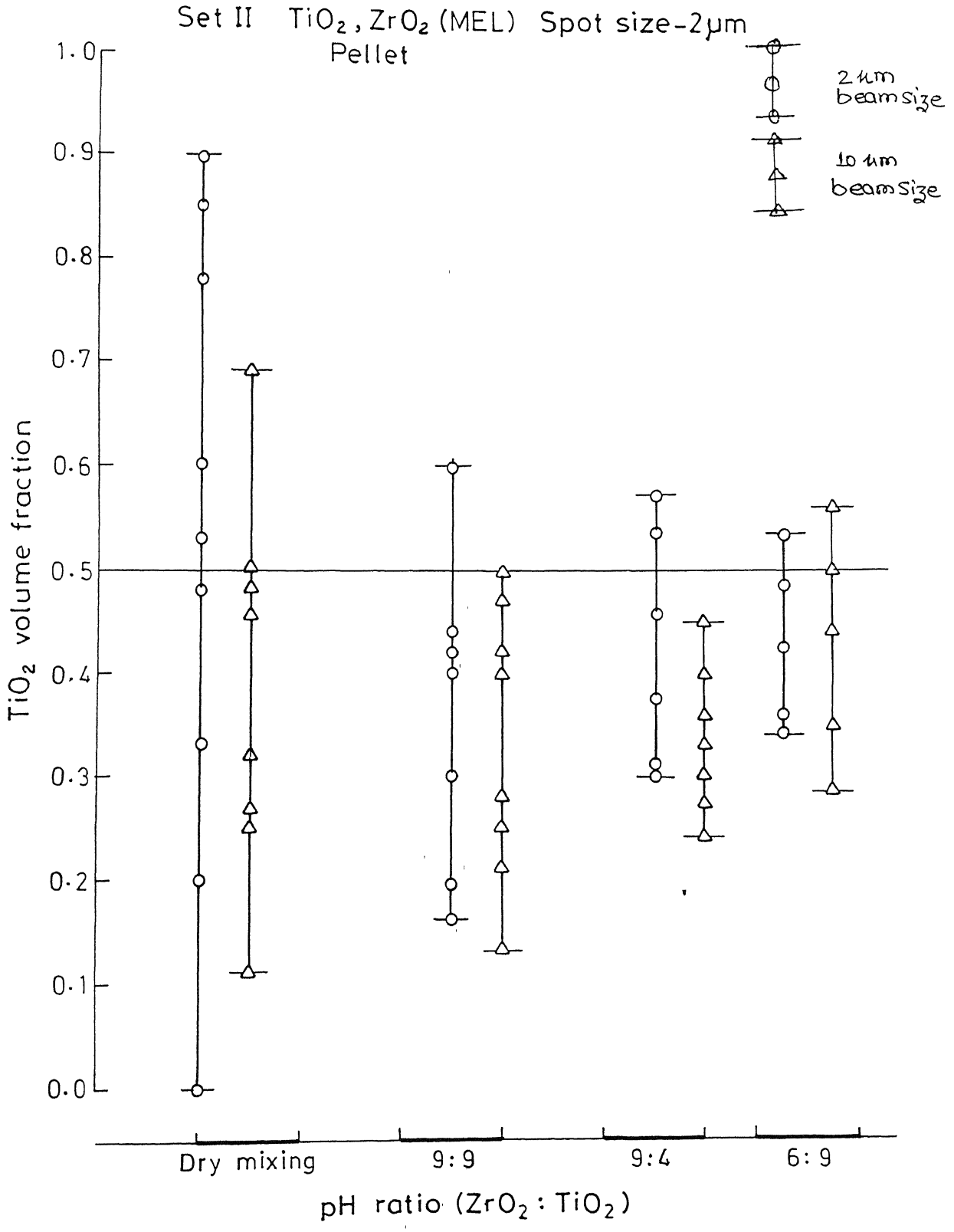

Fig (3.11): The plot showing volume fraction of TiO_2 at different mixing methods for

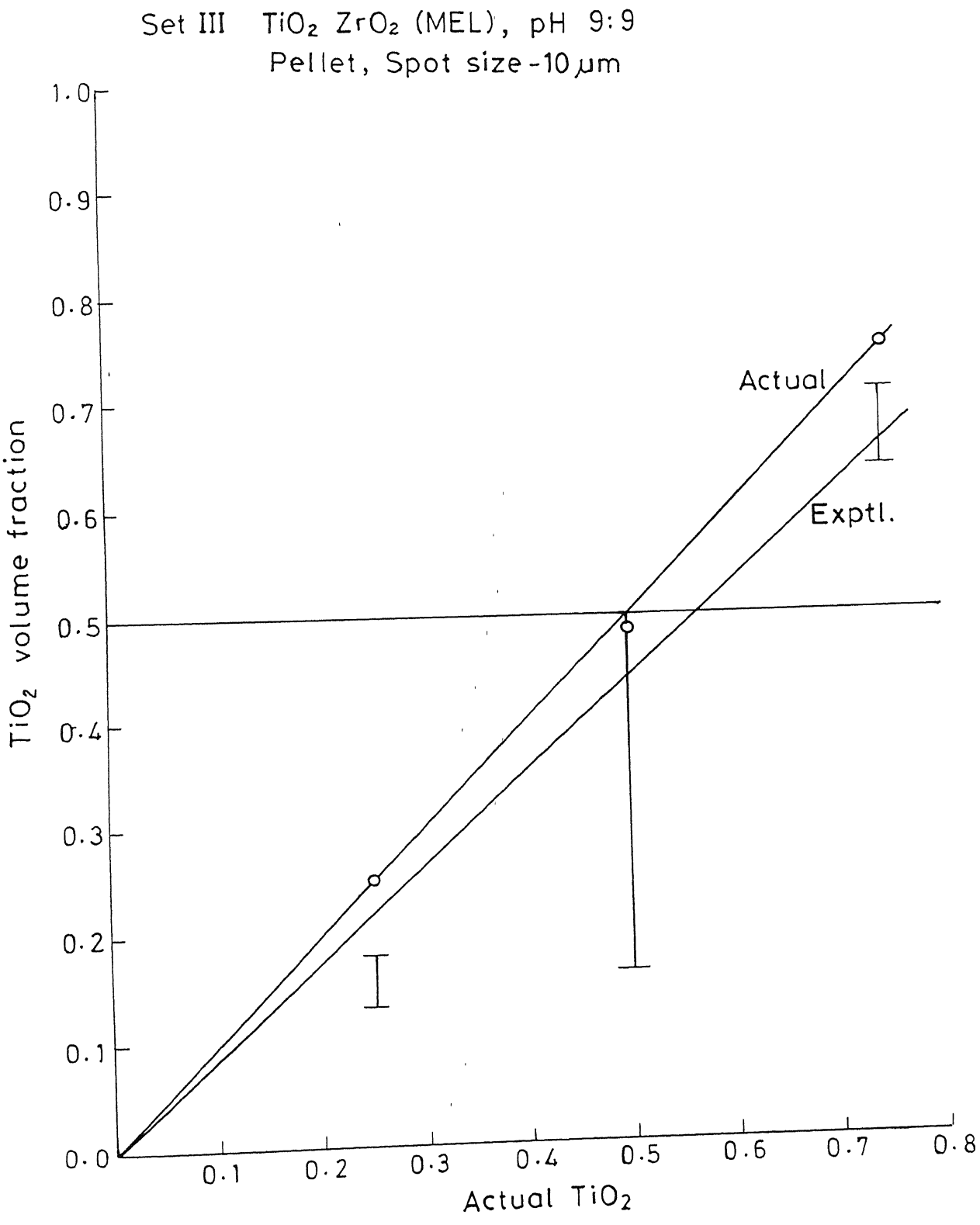

Fig (3.12): The plot showing volume fraction of Tio_2 at different mixing methods for

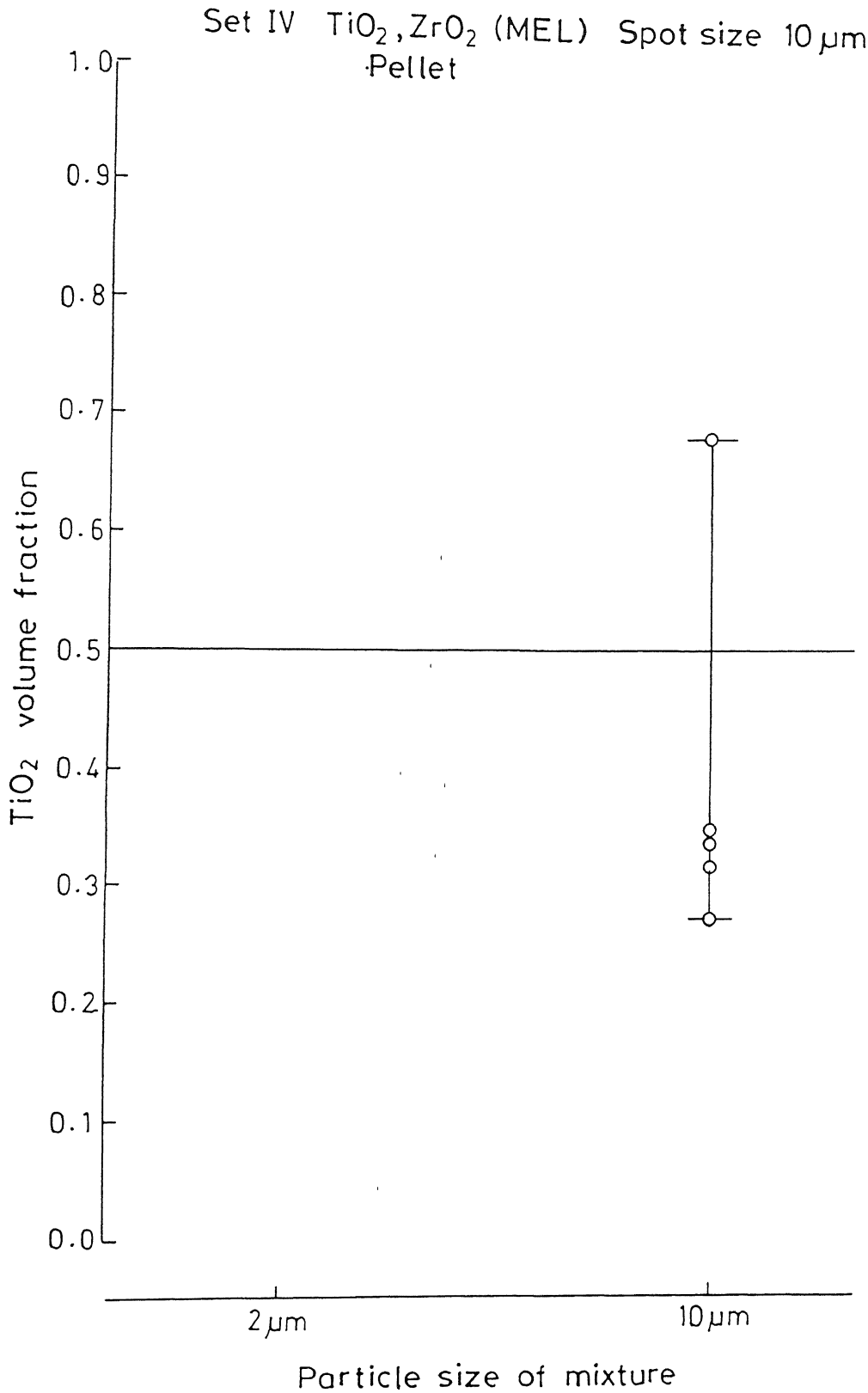

Fig(3.12a) The plot showing volume fraction of Tio_2 at different mixing methods for

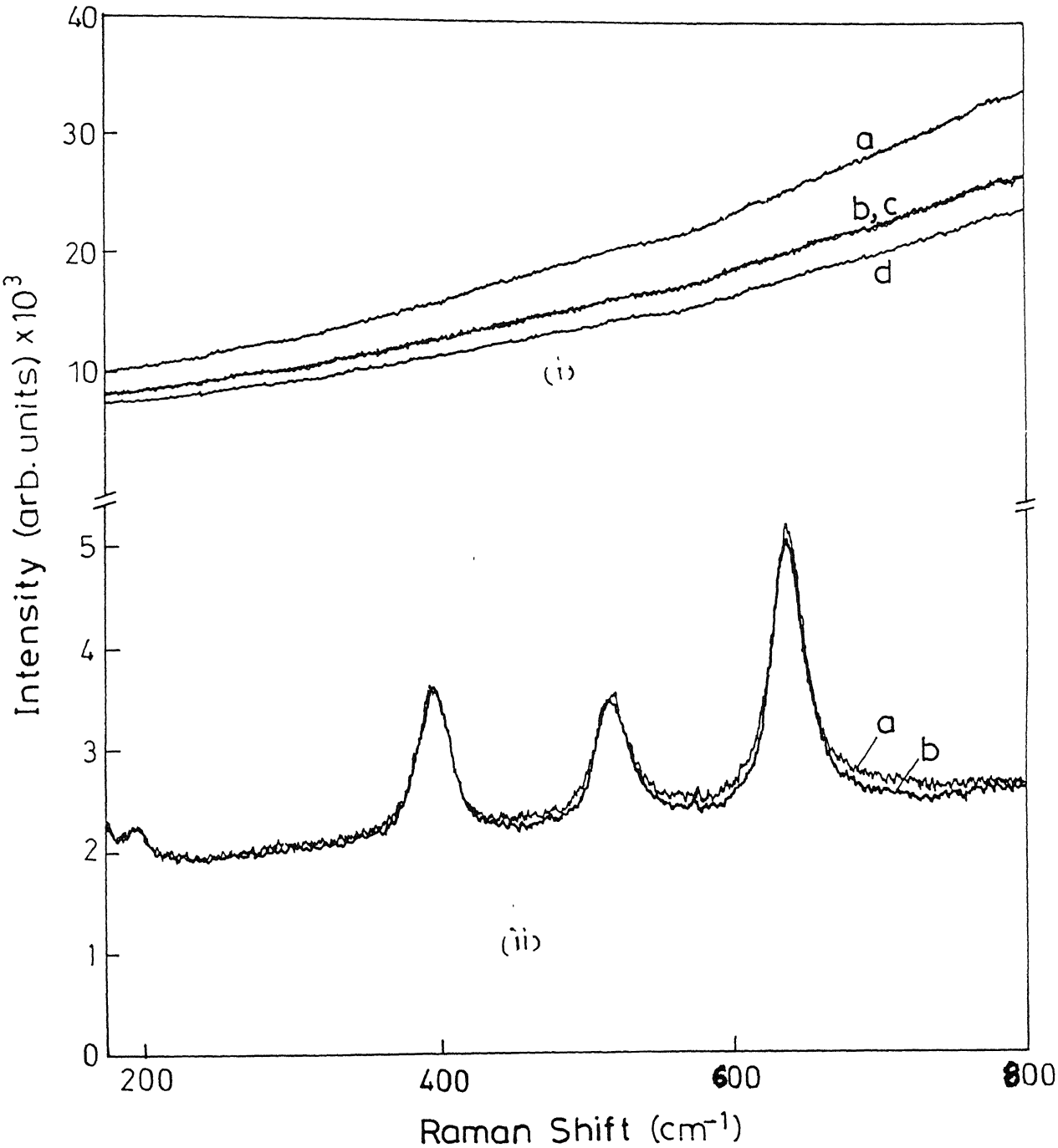

Fig(3.13): Raman Spectra of zro2 and Tio2 powders having particle size less than 2 μm(i) ZrO_2 (ii)TiO_2

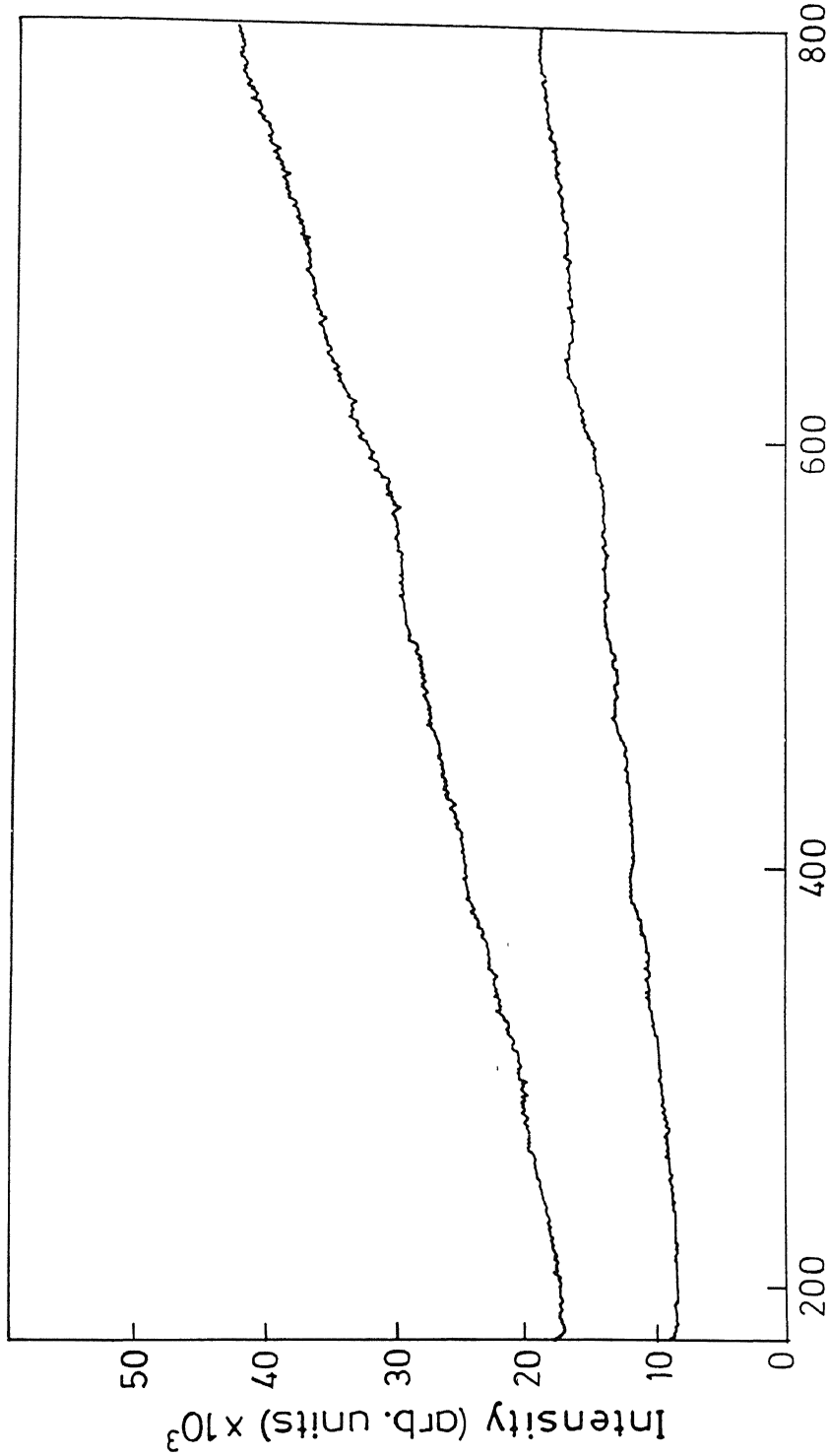

Fig (3 13 a) : Raman spectra of mixture of TiO_2 and ZrO_2 having particle size less than 2 μ m

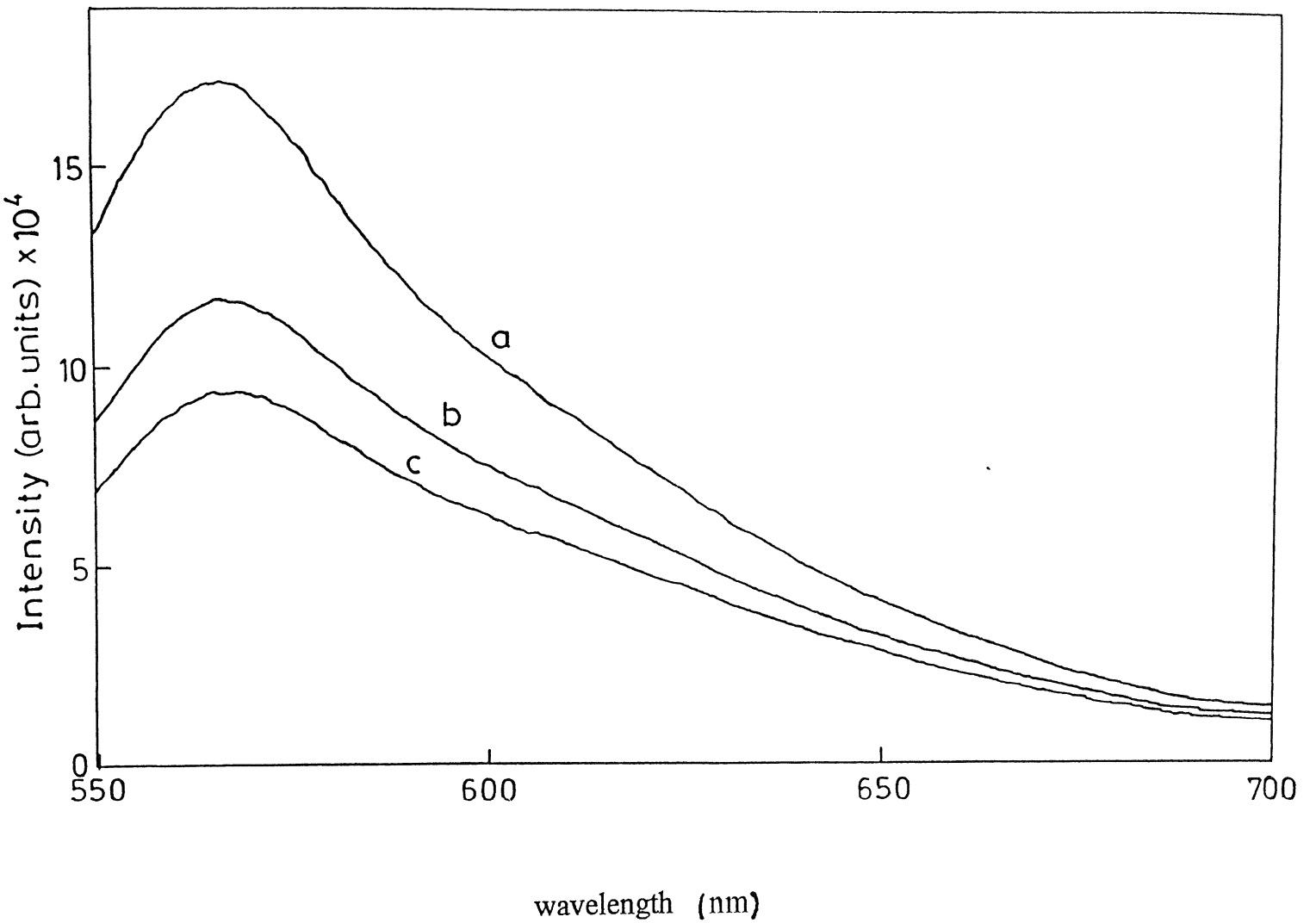

Fig (3.13b) Photoluminescence Spectra of ZrO_2 Powder (Particle size less than 10 μ m

DISCUSSION

From the above results the following points can be noticed:

(1) The volume fraction of TiO_2 determined experimentally is lower than the actual value in pellets and more than the actual value in samples made by pressing the powder between two glass slides. This can be seen from Figures (3.9) and (3.10)

(2) The scatter in the data is maximum in case of dry mixing as compared to the mixtures prepared using suspensions, which is as expected. Furthermore, it appears that mixing is better when the pH of the suspensions is 6:9 as compared to other pH. Fig. (3.9)

(3) In Fig. (3.10) the data using the beam sizes of 2 μm and 10 μm are compared. It is expected, that in the view of particle sizes being in μm range, the 10 μm beam size would give less scatter. For 2μm case, the scatter about the actual value is large as expected because 2μm beam size covers less surface area of the sample. However, for 10μm case, the scatter about the actual value is not as small as it should be. It was found that this arose from difficulty experienced in mounting the sample. This problem was later solved by using cubbet sample holder as can be seen from the small scatter in Fig. (3.11a and c).for 'a' and 'c' in fig (3.11) cubbet sample holder was used whereas 'b' in

fig (3.11) was taken without using cubbet sample holder which has given large scatter.

(4) Surprisingly, the scatter in the data using the 2 μm beam size for samples prepared by suspension is much less when the samples are prepared by pressing the powder between glass slides. (Fig.3.9)

(5) The striking difference between the results obtained from the samples pressed between glass slides (Fig.3.9) with regard to the TiO_2 volume fraction being consistently above and below the actual value of 0.486 respectively is not well understood. A possible scenario, which can result in the volume fraction of the finer powder(TiO_2) being observed, is be higher than the actual value is the first set of experiments is depicted in Fig (3.9.When this heap of powder is leveled by moving another slide to and fro over it, the larger particles are more likely to be pushed to the two ends, leaving a higher than average concentration of the finer particles in the central region from which the observations are taken. Thus the observed deviation towards higher TiO_2 concentration in the loose powder sample may be because of the sample preparation effect. However, this will need to be verified using powders of varying particle sizes.

The observed deviation (i.e. lower than the actual amount of TiO2) in the other set of experiments when

the pellet samples were used is not well understood. It appears that in the samples prepared using the powder in suspension, somehow the relative Raman scattering for the two types of powders is altered. For the analysis of data from these samples, the standard spectra obtained using the untreated pure powders were used. Hence, the change in the relative scattered intensity was not being automatically corrected and this may lead to observed deviation.

It should be noted that the TOSOH ZrO2 powder with coarser particle size was used for set I and finer MEL ZrO_2 powder for set II.The differences in particle sizes may also contribute to the observed differences. This is also supported by the data for the mixture containing all the particles more than 10μm as shown in fig (3.12). Further experiments are needed to understand these observations.

Conclusion

1 The scatter i.e. the variation in the composition from one point to another is found to be much more in the dry mixed samples as compared to the mixtures prepared from the suspensions.

2. Mixing of the powders is much better, when the pH of the starting material's suspension is 6 and 9 for ZrO2 and TiO2 respectively.

3. The loosed powder form gives more volume fraction than the actual value whereas pellet gives lower than the actual value.

4. The scatter in data is considerably reduced by using 10μ m beam size in comparison to 2μ m beam size.

5. The best mixing is obtained from the suspension in comparison to the dry mixed powders.

6. The reason for the more deviation in set 1 is discussed in the last chapter whereas the reason for the observed deviation in the other direction (i.e. lower than the actual amount of TiO_2) for the Set II when the pellet samples were used , are not well understood. It appears that in the samples prepared using the powders in the suspension, somehow the relative Raman scattering for the two types of powder is altered.

7. For the mixtures prepared using powders having particle sizes < 2μ m, the analysis couldn't be done as ZrO_2 particle size less

than 2 m shows photoluminescence which overcome the Raman scattering.

8. It is also seen that the topology of the powders affects the degree of mixing at different mixing techniques. The degree of mixing at localized regions depends on the particle size of the individual constituent.

Appendices

APPENDIX 1: CALCULATION OF AMOUNT OF TITANIA IN DIFFERENT VOLUME FRACTIONS

Let v be the volume fraction of TiO_2 desired in the mixture.

Then mass of TiO_2 and ZrO_2 in 1 ml of mixture is v x 3.9 gm and (1-v) 5.89 gm respectively.

Hence to obtain 5 ml of mixture,

Mass of TiO_2 powder (M_{Tio2}) = 5x 3.9xv

So, mass of ZrO_2 = (5- M_{TiO2}) gm

Using these relations, the masses taken and the corresponding volume fraction are shown in the Table1:

M_{TiO2} (gm)	M_{ZrO2} (gm)	V_{TiO2}
0.90	4.10	0.25
1.934	3.067	0.486
3.33	1.67	0.75

APPENDIX 2A: THE PROCESS OF BACKGROUND REMOVAL

The data file, which was obtained by renaming the text file, is used for background removal. The background is removed using PEAKFIT software as follows:

1 Choose the directory " as" containing the data files (*.dat)

C:\ > cd as

2 Call the "Peak fit" program

C:\ as>peak fit

3 Click File, Read data file, Standard. This will list all the files, and ask for the desired file.

Enter the desired file, press return.

4 Program asks, "Read multiple column data". Click No.

5 Program asks, "Use above titles?" Click Yes.

6 Go to EDIT

7 Bring the cursor to – ve values in data columns and delete them by "Ctrl Y"

8 Press F10 to save data

9 Press Escape

10 Go to "View" Option. Click "data graph". The plot will be displayed.

11 Press "Ctrl S". Two vertical lines appear. Take the left one to lower wave no. limit and click. Repeat for the higher limit of the wave no.

12 Go to Table Option in main menu. Choose the baseline subtract. A horizontal line will show up. Bring the line to touch the plot at the left

end, click. Now make the line (fixed at left end) to touch the plot at right and Click. Then press Enter.

13 Go to Table option. Click " Remove inactive". The system asks, " Save modified?" Click YES

14 A *. Prn file is obtained. Change it to text file by renaming

Rename _ *.prn_*. txt

15 Use the *.txt file for further processing by Excel.

APPENDIX 2B: COMMANDS TO CHANGE .SPT FILES TO .TXT FILES

1. Open the main menu by pressing F4; Main menu appears.
2. Click on the main menu; the menu appears as below:

Main Menu
Define Experiments
Display data
Process data
Create Hard Copy
Manage Files
Program Keystrokes
Set Defaults
Other Activities
Exit

3. Choose "Other Activities", the following choices appears

Label Data
SPEX Logo
ASCII Output
Input Nova File

4 Choose ASCII Output; Following choices appears:

Data File **********
Data Title **********
Output File **********
Go

5 Enter data filename, data title (date etc.), and output file name and click go.

References

1. M. J. Pelletier, "Introduction to Applied Raman Spectroscopy"; pp 1-2 . *Analytical Applications of Raman Spectroscopy*. Edited by M. J. Pelletier. Blackwell Science Ltd, Oxford 1999.

2. Nakashimo,S. and Hangyo,M. "Characterization of semiconductor Materials by Raman Microprobe," IEEE J. Quantum Electron, **25**(5), 965-975.

3. M. S. Dresselhaus, G. Dresselhaus, M. A. Pimenta, and P. C. Eklund, "Raman Scattering in Carbon Materials"; pp 368-378 in *Analytical Applications of Raman Spectroscopy*. Edited by M. J. Pelletier. Blackwell Science Ltd, Oxford 1999.

4. J. B. Cooper, "Process Control Applications for Raman Spectroscopy in the Petroleum Industry"; pp 193-195 in *Analytical Applications of Raman Spectroscopy*. Edited by M. J. Pelletier. Blackwell Science Ltd, Oxford 1999.

5. M. Gotic, M. Ivanda, S. Popovic, S. Music, A. Seculic, A. T. Urkovie and K. Furic, "Raman Investigation of Nanosized Titania," *J. Raman Spec.* Vol **28**, 555- 558 (1997).

6. S. Karlin and Ph. Colomban, "Raman Study of the Chemical and Thermal Degradation of as Received and Sol-Gel Embedded Nicalon

and Hi-Nicalon SiC Fibers Used in Ceramic Matrix Composites," *J. Raman Spec.* Vol **28**, 219- 228 (1997).

7. Huo Chang and Pei Jane Huong, "Thermo Raman Studies of Anatase and Rutile TiO_2," *J. Raman Spec.* Vol **29**, 97- 102 (1998).

8. J. F. Meng, P. S. Dobal, R. S. Katiyar and G. T. Zou, "Optical Phonon Modes and Phase Transition in the $Bi_4Ge_{3-x}Ti_xO_{12}$ Ceramic System," *J. Raman Spec.* Vol **29**, 1003-1008 (1998).

9. C. Y. Wang, Z. X. Shen and B. V. R. Chowdhari, "Raman Studies of $Ag_2OWO_3TeO_2$ Ternary Glasses," *J. Raman Spec.* Vol **29**, 819- 823 (1998).

10. Patrice Huguet and Robert Gaufres, "Determination of the Temperature of the Gas by a Simple and Accurate Raman Method," *J. Raman Spec.* Vol **26**, 327- 329 (1995).

11.M. N. Iliev, V. G. Hadjiev and V. G. Ivanov, "Raman Spectroscopy of Low Structure and Recording Processes in $YBa_2Cu_3O_{7-\delta}$ Type Compounds," *J. Raman Spec.* Vol **27**, 333- 342 (1996).

12. S. B. Majumder, V. N. Kulkarni, Y. N. Mohapatra and D. C. Agrawal, "Micro Raman Spectroscopy of Sol-Gel Derived $Pb(Zr_xTi_{1-x})O_3$ Thin films," *J. Raman Spec.* Vol **24**, 459- 462 (1993).

13. Paul R. Mort, Richard E. Rimon, "Determination of Homogeneity Scale in Ordered and Partially Ordered Mixtures," *Powder Technology*, **82**, 93- 104 (1995).

14. M. Poux, P. Fayolee, J. Bertrand, D. Briduox and J. Bousquet,

"Powder Mixing: Some Practical Rules Applied to Agitated Systems," *Powder Technology*, 68, 213- 234 (1991).

15. P. M. C. Lacey, "Developments in the Theory of Particle Mixing," *J. Appl. Chem.*, **4**, May 1954.

16.A.Lelan "A proposed Universal Homogenity and Mixing Index"Ing. A 10 (1989) A5940

17. James S. Reed, "Introduction to the Principles of Ceramic Processing," pp. 143, John Wiley and Sons, NY.

18. P. S. Dobal, "GaAs System and Oval Defects: A Laser Spectroscopic Study," PhD Thesis, Dept. of Physics, Indian Institute of Technology, Kanpur (1980).

19. Instruction and Operating Manual HX Refrigerated Recirculating Heat Exchanger (NESLAB USA).

20.Operation and Maintenance Instructions, 1877E Triplemate (SPEC Industries, NJ, USA).

21.D. F. Barbe, Proceedings of IEEE, **63**, 38 (1975).

22. T. Ohsaka, S. Yamaoka and O. Shimomuro, "Effect of Hydrostatic Pressure on the Raman Spectrum of Anatase (TiO_2)," Solid State Communications, vol **30**, no. 6, pp 345- 347.

23. C. G. Kontoyannis, G. Carountzos, "Quantitative Determination of the Cubic to Monoclinic Phase Transformation in Fully Stabilized Zirconias by Raman Spectroscopy," *J. Am. Ceram. Soc*, 77[8]

2191-2194 (1994).

24.E. E. Underwood, "The Mathematical Foundation of Quantitative Stereology," pp 5 in "Stereology and Quantitative Metallography," ASTM STP No. 504, American Society for Testing and Materials, PA, 1972.

-133084

Date Slip

The book is to be returned on the date last stamped.

.....	.....
.....	.....
.....	.....
.....	.....
.....	.....
.....	.....
.....	.....
.....	.....
.....	.....
.....	.....
.....	.....
.....	.....